NASA TECHNICAL NOTE

NASA TN D-4597

c.1

CHARACTERISTICS AND USE
OF X-15 AIR-DATA SENSORS

by Lannie D. Webb

Flight Research Center
Edwards, Calif.

CHARACTERISTICS AND USE OF X-15 AIR-DATA SENSORS

By Lannie D. Webb

Flight Research Center
Edwards, Calif.

NATIONAL AERONAUTICS AND SPACE ADMINISTRATION

CONTENTS

CHARACTERISTICS AND USE OF X-15 AIR-DATA SENSORS

By Lannie D. Webb
Flight Research Center

SUMMARY

The uses, techniques of correlation, and analysis of flight-guidance and air-data sensors that have been flown on the X-15 airplane are examined. Methods by which meteorological balloons and high-altitude rocketsondes were used to define the atmospheric envelope around the X-15 airplane are discussed. The application of onboard sensor data, meteorological data, and radar data in obtaining altitude, velocity, Mach number, and dynamic pressure is explained.

Onboard systems considered are the nose-boom pitot-static tube, hypersonic flow-direction sensor (ball nose), fuselage static system, fuselage pitot probe, stagnation-temperature probe, and inertial flight-data system. Flight experience and data analysis show that the nose-boom pitot-static tube has a small position error and is relatively insensitive to angles of attack up to 12°. By using the hypersonic flow-direction sensor, stagnation pressure can be measured accurately over large angle-of-attack (-20° to 40°) and angle-of-sideslip (±20°) ranges. Static-pressure orifices on the fuselage of the X-15 airplane were very sensitive to changes in angle of attack above a Mach number of 1. The fuselage static-pressure orifices have a large position error which changes with angle of attack and makes altitude and Mach number difficult to measure. A stagnation-temperature probe was used on a limited number of X-15 flights to obtain indirect free-stream velocity measurements up to 6000 ft/sec. For dynamic pressures between 100 lb/ft^2 and 1000 lb/ft^2, the velocity derived from the temperature probe differed by 3 percent on the average from radar velocity. Velocity errors became large when dynamic pressures decreased below 100 lb/ft^2 and were attributed to radiation errors. The inertial-altitude errors increased exponentially with time after launch and were usable only for the first 300 seconds for most flights. For these conditions the accuracy of the altitude presented to the pilot was within ±5,000 feet.

INTRODUCTION

Flight research with experimental aircraft requires precise control and knowledge of the vehicle's velocity, altitude, attitude, and the atmospheric environment through which it is flying. The wide extremes of environmental and aerodynamic conditions encountered during research flight with the X-15 airplane exceeded the capabilities of existing measurement systems, thus new techniques and sensors had to be developed.

For the initial low-speed flights of the X-15 airplanes, a conventional nose-boom pitot-static sensing tube with vane-type angle-of-attack and angle-of-sideslip sensors was used. As the flight speeds approached a Mach number of 4, this tube was removed

and replaced with a hypersonic flow-direction sensor, commonly referred to as the ball nose, which was designed to withstand the stagnation temperatures encountered at the higher speeds. However, because of the mechanical complexity of the ball nose and the possibility of failure and because the ball nose does not provide a satisfactory static-pressure sensor, a second system consisting of a fuselage-mounted "dog-leg" pitot probe and fuselage static orifices was also installed to insure adequate information for the pilot during landing. Inasmuch as none of these systems function in the rarefied atmosphere at the higher altitudes of which the X-15 airplanes are capable, the vehicles have also been provided with an inertial system to give the pilot information necessary during portions of such flights. A stagnation-temperature probe is also used on some flights to evaluate its ability to provide Mach number indications in certain speed ranges.

In addition to the vehicle-mounted sensors, ground-based radars are used to determine the velocity and altitude of the airplane on all flights. These data in conjunction with meteorological sounding data permit the determination of dynamic pressure and Mach number independently of the airplane systems. The radar and sounding data thus provide information with which to determine calibrations and flight response characteristics of the onboard guidance sensors.

Almost 200 X-15 flights have been made, and the redundancy of the various air-data systems has made it possible to assess the accuracy and other characteristics of each system. This paper describes the systems and assesses their performance.

SYMBOLS

Only symbols used in the text are defined in this section. Symbols used in the appendixes are defined therein.

a_n	normal acceleration, g units
a_x, a_y, a_z	three-axis component accelerations, g units
g	gravitational acceleration, 32.15 ft/sec^2
H	ambient enthalpy units, Btu/lb
H_o	stagnation enthalpy units, Btu/lb
h'	indicated pressure altitude, ft
h_i	inertial altitude above mean sea level, ft
h_r	geometric altitude (radar altitude above mean sea level), ft
$h_{r,f}$	faired geometric altitude, ft

Δh_p	error in standard pressure altitude due to static-pressure error, $h_{r,f} - h'$
J	mechanical equivalent of heat, 778 ft-lb/Btu
K	constant, $\dfrac{q'_p}{p_{t_2}}$, 0.526 or 0.540
M	free-stream Mach number
M'	indicated Mach number
ΔM	Mach number error, $M - M'$
p	free-stream ambient pressure, lb/ft^2
p'	indicated ambient pressure, lb/ft^2
p_{t_2}	ball-nose or nose-boom stagnation pressure, lb/ft^2
p_{t_3}	fuselage-pitot-probe local stagnation pressure, lb/ft^2
p_{70}	ball-nose indicated static pressure (70° port), lb/ft^2
p_α	ball-nose angle-of-attack pressure, lb/ft^2
q	dynamic pressure, lb/ft^2
q_c	true impact pressure, $p_{t_2} - p$, lb/ft^2
q'_c	indicated impact pressure, $p_{t_2} - p'$, lb/ft^2
q'_p	q-meter indicated dynamic pressure, lb/ft^2
t	time, sec
V_r	radar velocity (corrected for winds), ft/sec
$V_{r,f}$	faired radar velocity (corrected for winds), ft/sec
V_{st}	temperature-probe flow velocity, ft/sec

X, Y, Z	rectangular coordinate axis
α	angle of attack, deg
γ	specific-heat ratio, 1.4
ϵ	temperature-probe recovery factor, 0.996
σ	standard deviation

Subscript:

| max | maximum |

RADAR AND METEOROLOGICAL SOUNDINGS

Radar Measurements

The X-15 rocket-powered airplane (fig. 1) is capable of covering a ground range of approximately 300 nautical miles while simultaneously passing through a wide portion of the earth's sensible atmosphere after being launched from a B-52 airplane. Figure 2 shows the test altitude range and the atmospheric layers traversed, and the standard-day variation of temperature and density for the various atmospheric layers. The flight performance envelope extends to hypersonic Mach numbers in excess of 6 and to altitudes greater than 350,000 feet.

To monitor a flight envelope of this magnitude required the establishment of a radar tracking range (commonly referred to as High Range) consisting of three radar ground stations (fig. 3(a)). The radar station at the NASA Flight Research Center, Edwards, Calif., acts as the prime control during an X-15 flight. The Edwards control room (fig. 3(b)) receives real-time velocity and altitude from the three radar stations. The altitude and ground track are displayed on large plotting boards, and the velocity is indicated on a meter for the ground controller's use. Radar data are also recorded in digital form and are later corrected to free-stream values by using weather data obtained from balloon and rocket measurements. The corrected radar data are used as the standard for X-15 data analysis.

Mod II radars (modified SCR-584 radars) are used at all stations. This type of radar is an automatic angle and range-tracking system designed to provide azimuth, elevation angle, and slant-range data. The radars operate on S-band and have a 400-mile range capability. Tracking information in the form of azimuth, elevation, and range is obtained from two optical encoders and one electromechanical encoder (range) attached directly to the radar antenna and range shafts. A 16-digit parallel code is obtained for azimuth, elevation, and slant range at a rate of 10 samples per second. This digital information from the encoders is recorded on magnetic tape.

The radar data are reduced to yield velocity, altitude, and other parameters. In the data-reduction process, discussed in detail in appendix A, information from all three stations is smoothed by applying a least-square weighted polynomial curve fit of the second degree. Figure 4(a) indicates the characteristics of the unsmoothed and smoothed velocity and altitude data. Figure 4(b) illustrates the effect of the smoothing in areas where radar data are completely lost. The lost-data area is partially filled

by smoothing the data preceding the data dropout. Corrections for radar-antenna offset and atmospheric refraction (ref. 1) are made in the calculation deck. Elevation-angle corrections are based on surface observations of atmospheric properties at the radar sites (appendix B). The data are then converted from spherical to X, Y, and Z rectangular coordinates. Altitude is computed for a spherical earth, using the earth's radius of curvature at the latitude of the tracking station. Next, the data are differentiated for velocity over the entire run. Finally, atmospheric wind corrections are added to resolve the aircraft's velocity to free-stream values.

Balloon Soundings

Onboard measurements of ambient atmospheric conditions are difficult to make because of the flow field around the X-15 aircraft. Consequently, meteorological sounding data are used to correct radar data in order to obtain free-stream conditions. These data are used to calculate free-stream velocity, Mach number, and dynamic pressure. For example, radar velocity is corrected to free-stream values by adding or subtracting horizontal wind components.

Balloon sounding data are used from the ground surface to an altitude of approximately 100,000 feet. Data from the balloon soundings are extrapolated beyond 100,000 feet for X-15 flights that do not exceed about 125,000 feet.

For each X-15 flight an AN/AMT-4B rawinsonde balloon (ref. 2) is released by the Air Force Air Weather Service, Edwards Air Force Base, Calif., as the B-52 launch airplane takes off. The radiosonde package transmits signals which are received by an AN/GMD-1A rawin set (ref. 3). These data are recorded on magnetic tape for subsequent data reduction (ref. 4).

Sounding Rockets

For X-15 flights above 100,000 feet altitude, meteorological sounding rockets provide data on prevailing winds. The winds between 100,000 feet and 200,000 feet are monsoonal during the winter (October 1 to March 15) with strong westerly flow. From June 1 to August 15 the prevailing winds are weaker and are easterly. Between these two periods, there are short transitional periods of weak and variable winds (ref. 5).

The wind data for X-15 flights are obtained from LOKI (HASP) and ARCAS meteorological sounding rockets fired from the Tonopah (Nev.) Test Range of the Atomic Energy Commission and from the Point Mugu (Calif.) Naval Air Station. The geographic relationship of the X-15 flight path and the launching sites of the sounding rockets is shown in figure 5. LOKI wind soundings are made by radar tracking of metalized-nylon chaff. ARCAS wind soundings (ref. 6) are obtained by tracking a parachute that opens at an altitude of about 200,000 feet. Wind data above 200,000 feet are extrapolated from the lower-altitude data. The solid line in figure 6 shows a set of temperature and wind profiles used for an X-15 flight.

The ARCAS parachute package carries a 10-mil bead thermistor for measurement of ambient temperatures. Data from this temperature sensor are used up to about 150,000 feet. Above this altitude the data are of doubtful validity (ref. 7).

5

Above 200,000 feet all pressure and temperature values for X-15 flights are obtained from standard atmospheres (refs. 8 to 10) because of a lack of meteorological data. The integration of standard atmospheric values with meteorological balloon and rocket measurements is only a partial solution but has been satisfactory for the X-15 airplane.

The high-altitude capability of the X-15 aircraft has created difficulties in interpreting Mach number because sound transmission becomes meaningless, as a result of the rarefied atmosphere, and the correct value of the free-stream specific heat ratio γ is difficult to determine. An altitude of 300,000 feet has been proposed as the lower limit of space as a result of these problems (ref. 11). The values of Mach number for X-15 flights above 300,000 feet have been calculated, with reservation, by assuming the specific-heat ratio to be a constant (1.4).

DESCRIPTION OF ONBOARD GUIDANCE SENSORS

Nose-Boom Pitot-Static Tube

A standard NACA pitot-static tube (fig. 7) was selected to obtain velocity, altitude, and flow-direction data for the initial (low Mach number) X-15 flights. The probe was mounted on a nose boom ahead of the X-15 fuselage (fig. 8) to minimize fuselage interference effects on the static-pressure orifices. Static-pressure orifices were located approximately 7.9 inches (9 tube diameters) behind the nose of the pitot-static tube (ref. 12) and 63 inches forward of the tip of the nose of the aircraft. Wind-tunnel data show that the error in the stagnation pressure p_{t_2} is less than 1 percent over an angle-of-attack range from -13° to 32° for this probe (ref. 13).

Mach number, velocity, and pressure altitude were obtained from true impact pressure q_c and ambient pressure p. Static pressure was corrected for position error. Mach number was calculated by using the expression

$$\frac{q_c}{p} = \left(1 + \frac{\gamma - 1}{2} M^2\right)^{\frac{\gamma}{\gamma - 1}} - 1 \tag{1}$$

for Mach numbers less than 1 and the Rayleigh pitot formula

$$\frac{q_c}{p} = \frac{1 + \gamma}{2} M^2 \left[\frac{(1 + \gamma)^2 M^2}{4\gamma M^2 - 2(\gamma - 1)}\right]^{\frac{1}{\gamma - 1}} - 1 \tag{2}$$

for Mach numbers greater than 1. The pitot-probe Mach number and calibrated static pressure were used to calculate dynamic pressure from the relationship

$$q = \frac{\gamma}{2} M^2 p \tag{3}$$

Hypersonic Flow-Direction System (Ball Nose)

High stagnation temperatures, resulting from the enlargement of the X-15 flight region beyond a Mach number of 3, required the removal of the pitot probe and nose boom. A high-temperature flow-direction system (ball nose) was installed on the nose of the airplane (fig. 1). The sensor's primary purpose was to measure angle of attack and angle of sideslip (ref. 14) by moving to null out pressure differences on the sphere encountered during flight. A secondary use was the measurement of stagnation pressure by using an orifice which always senses stagnation conditions.

The sensor consists of a 6 1/2-inch-diameter movable sphere partly housed within a 16 3/4-inch-long truncated cone (fig. 9(a)). The internal temperature of the sensor is controlled by a cooling system that utilizes liquid nitrogen. The sphere is hydraulically actuated and is an electronically controlled servomechanism, as illustrated for the pitch plane (yaw plane is similar) in figure 9(b). Differential pressures between opposing sphere-surface orifices (two in the pitch plane and two in the yaw plane) are converted, by pressure transducers, to electrical signals. The hydraulic actuators move the sphere to a zero differential pressure which brings the ball-nose stagnation-pressure orifice to the stagnation point of the flow. Angle of attack (-20° to 40°) and angle of sideslip (±20°), referenced to the centerline of the airplane, are indicated by the nulled position of the sphere. This position is detected by a synchro transmitter and relayed to the ground monitoring station, as well as recorded onboard.

The hypersonic flow-direction system has been used for purposes in addition to the basic required measurements of angle of attack, angle of sideslip, and impact pressure for airspeed. A static-pressure orifice 70° away from the free-stream flow on the nulling sphere (fig. 9(b)), along with the stagnation-pressure orifice, can provide measurements of Mach number and pressure altitude independent of angle of attack (ref. 15) up to a Mach number of about 4.5. Stagnation pressure measured from the stagnation orifice of the sphere has been used to determine atmospheric density for altitudes up to approximately 200,000 feet (refs. 16 and 17). Stagnation pressures have also been used extensively in determining dynamic pressure. By substituting equation (3) into equation (2) and rearranging terms, the following expression is obtained:

$$q = \frac{\gamma}{\gamma + 1} \left[\frac{4\gamma}{(\gamma + 1)^2} - \frac{2(\gamma - 1)}{(\gamma + 1)^2 M^2} \right]^{\frac{1}{\gamma - 1}} p_{t_2}$$

For $M \geq 1$ and $\gamma = 1.4$ the equation reduces to

$$q = \frac{1}{1.84} \left(1 - \frac{1}{7M^2} \right)^{2.5} p_{t_2} \qquad (4)$$

Pilot's q-Meter

At the higher Mach numbers, dynamic pressure is primarily a function of stagnation pressure. Accordingly, a real-time presentation of dynamic pressure was obtained by connecting the stagnation-pressure orifice of the ball nose to a modified Mach meter in the X-15 cockpit (fig. 10). The modified Mach meter contained only an

absolute-pressure cell (0 to 4800 lb/ft^2). The face of the meter was modified so that dynamic pressure could be read directly.

Figure 11 shows the ratio of dynamic pressure to ball-nose stagnation pressure as a function of Mach number. As can be seen from the figure, the influence of Mach number in equation (4) is small for high Mach numbers (M > 2). Consequently, dynamic pressure becomes almost completely dependent on stagnation pressure alone. The ball-nose stagnation-pressure orifice affords excellent stagnation-pressure measurements which are used in conjunction with radar-determined Mach number in equation (4) to calculate dynamic pressure.

Fuselage Static System

The ball-nose installation created a need for static-pressure orifices to replace the static orifices located on the pitot-static tube. Thus, two manifolded static-pressure orifices were placed on opposite sides of the fuselage 2 inches above the centerline of the aircraft and 50 inches aft of the leading edge of the ball nose (fig. 12). These orifice locations provided acceptable static-pressure measurements over the speed and attitude ranges of X-15 landings. The static-pressure orifices were connected to a diaphragm-type absolute-pressure recorder and to the pilot's altimeter for measurement of indicated ambient pressure p'. The fuselage static-pressure orifices were also coupled to the ball-nose stagnation-pressure orifice by means of a diaphragm-type differential-pressure recorder to measure indicated impact pressure q_c'. The ratio of $\dfrac{q_c'}{p'}$ was used along with the Rayleigh pitot equation to obtain indicated Mach number.

Fuselage Pitot Probe

Because of the possibility of the ball nose becoming inoperative during a research flight, a pitot probe (fig. 13) was mounted 70 inches aft of the leading edge of the ball nose of the X-15. The pilot's airspeed indicator was connected between the stagnation-pressure orifice of the pitot probe and the fuselage static-pressure orifices. Although primarily used for landing, the airspeed indicator has occasionally been used by the pilot during flight at low supersonic speeds.

Figure 12 shows the relationship of the fuselage pitot probe to all the airspeed sensors that have been used on the X-15 airplane.

Stagnation-Temperature Probe

A stagnation-temperature probe has been tested on the X-15 airplane as a secondary technique for measuring free-stream velocity (ref. 18). The probe was mounted on the leading edge of the left wing tip (fig. 14(a)). The system consists of two thermocouples, a reference oven, and an oscillograph (fig. 14(b)). The probe thermocouple is housed in a radiation shield composed of three concentric tubes (fig. 14(b)). The shields and support were designed to reduce the loss of heat by conduction and radiation. To replenish some of the energy lost through conduction and radiation from the

thermocouple junction to the walls, a flow of air was allowed through small vent holes in the outer shield (ref. 19).

The probe was designed to have less than 2-percent error for the following conditions:

Mach numbers from 3 to 5

Stagnation temperatures less than 2400° R

Stagnation pressures greater than 600 lb/ft^2

The temperature probe had the dual purpose of providing recorded stagnation-temperature data for later analysis and presenting velocity to the pilot during flight. For the latter purpose, an average value of ambient temperature had to be selected. A value of 400° R was chosen after examining X-15 flight conditions for which cockpit presentations of velocity were needed. This value was used to calibrate the probe. To compensate for the heat losses, a recovery factor ϵ of 0.996 was assumed. For the high stagnation temperatures encountered during an X-15 flight, ideal-gas relationships for analysis of the data from the stagnation-temperature probe were considered inappropriate. Measured stagnation temperatures and the assumed ambient temperature were converted to enthalpies from tables in reference 20 and used to calculate velocity from the following equation (from ref. 21):

$$(H_O - H) = \frac{\epsilon}{2gJ} (V_{st}{}^2)$$ (5)

Equation (5) is an energy relationship that assumes thermal equilibrium and accounts for the energy loss.

The stagnation-temperature probe was connected to a self-balancing potentiometer in the X-15 cockpit. The meter was calibrated by first determining the millivolt output of the stagnation-temperature probe as a function of temperature. Next, the same voltage was applied to the potentiometer in the cockpit and the face of the meter marked in terms of the velocity corresponding to temperature. Thus, the free-stream velocity of the aircraft becomes solely a function of stagnation temperature.

A deviation of 70° R in atmospheric temperature from the assumed 400° R will produce a 100 ft/sec error in cockpit velocity at $M = 5$. For later analysis, the velocity error can be reduced by correlating the true ambient temperature with altitude on the day of the flight.

Inertial Flight Data System

The X-15 sensors discussed in the preceding sections were dependent on the surrounding environment (for example, pressure and temperature) for their operation. The inertial flight data system is unique in that it is independent of the atmosphere. The system functions by sensing the vehicle's acceleration and calculating in flight the change of velocity and position from the initial conditions. The force acting on each of the accelerometers of the inertial system has a gravitational and nongravitational component.

Figure 15(a) summarizes the major system components of the B-52 supporting equipment and the X-15 inertial system. The major X-15 components are the inertial measurement unit, the computer, and the pilot's display. The inertial measurement unit (IMU) contains a four-gimbal system to provide complete attitude freedom in all axes and utilizes three force rebalance accelerometers and three single-degree-of-freedom gyroscopes. A direct-current analog computer is used to convert the IMU information into velocity and position data. The computer also performs the erection and alinement function in conjunction with the B-52 control panel.

The X-15 inertial flight data system is alined on the ground to local level and the X-15 High Range azimuth. It maintains this orientation throughout the flight (fig. 15(b)). Vehicle Euler attitudes, inertial velocities, and altitude are determined by the inertial system and correlated with the time and position of X-15 launch for later data analysis. The inertial display (fig. 10) for the pilot contains: a three-axis attitude ball with a deviation-from-flight-path indicator, an inertial-velocity indicator, an inertial altimeter, and an inertial rate-of-climb meter.

During the pre-launch phase (erection), an AN/APN-81 Doppler radar is used as a horizontal-velocity reference (erection) for the IMU. An N-1 compass is used during the straight and level portions of the captive flight for the heading reference. The B-52 pressure altimeter provides the reference altitude for the platform at launch. Radar altitude is used to correct the inertial altitude just before launch.

After launch with the system in the inertial mode, a Schuler tuned circuit oscillator (ref. 22) is used to maintain the stable platform perpendicular to an imaginary line passing through both the platform and the earth's center. Use of the Schuler oscillation also results in errors in the horizontal navigation channel being self-limiting. However, the vertical-channel errors are unbounded and increase exponentially with time (ref. 23).

The inertial system was designed to provide the X-15 with fairly accurate altitude data for the first 300 seconds of flight only. The following table summarizes the inertial-measurement specifications for the first 300 seconds of an X-15 flight:

Measurements required	Range	Accuracy (root mean square)
Attitude angles, deg	Unlimited*	0.5
Height, ft	0 - 500,000*	5,000
Velocity, ft/sec		
Total	7,000*	70
Down range	±7,000*	50
Cross range	±3,000*	50
Vertical	±5,000*	20

*Required for pilot displays.

Limitations on the volume of the inertial system were the prime considerations in design and precluded a system that could maintain a bounded error in altitude from B-52 take-off to X-15 landings, a period of about 600 seconds to 700 seconds.

10

After launch of the X-15, the ground controller transmits the elapsed time, radar altitude, and radar velocity to the pilot for comparison with the cockpit inertial data. Use of radar quantities during the flight enables the pilot to check the performance of the inertial system and establish the credence that should be placed on the cockpit readings.

RECORDING APPARATUS

Pressures measured by the nose-boom pitot-static tube, fuselage pitot probe, ball-nose sensor, and fuselage static system were recorded on a standard NACA aneroid airspeed recorder. The recorder was located in the nosewheel compartment, 34 inches rearward of the hypothetical tip of the X-15 ogive nose. Each NACA airspeed recorder provides space for four pressure-recording cells of variable pressure ranges. Two of the four NACA aneroid pressure-recording cells were absolute-pressure cells (0 to 2200 lb/ft^2 and 0 to 212 lb/ft^2); the other two were differential-pressure cells (0 to ±2600 lb/ft^2 and 0 to ±212 lb/ft^2). The smaller-range absolute- and differential-pressure cells were used in order to obtain more accurate pressure data at high altitudes. Impact-pressure and indicated ambient-pressure measurements were obtained by using differential- and absolute-pressure cells, respectively, for the nose-boom pitot-static and ball-nose configurations.

The accuracy of the NACA aneroid airspeed recorders is ±0.25 percent of full-scale (ref. 24). For the primary combination of differential- and absolute-pressure cells (0 to 2600 lb/ft^2 and 0 to 2200 lb/ft^2) that are used to obtain airspeed, the root-mean-square measurement uncertainty would be approximately ±8.5 lb/ft^2.

The outputs of the stagnation-temperature probe and the inertial flight data system were recorded onboard by a 36-channel oscillograph. The cockpit instruments were photographed by a 16-mm camera positioned on the right side of the canopy.

DISCUSSION OF CHARACTERISTIC AND CALIBRATION ERRORS

Radar and Meteorological Soundings

Each of the three Mod II radars has a pointing uncertainty of approximately ±2 mils in elevation and azimuth and ±120 feet in slant range (ref. 25). A ±2-mil pointing uncertainty produces a cone of altitude uncertainty, which increases with the object's slant-range distance from the tracking station. For example, an object being tracked by the Edwards Mod II radar would have altitude uncertainties of ±3500 feet or ±1600 feet, depending on whether it was over Ely or Beatty. Other contributing errors in the radar measurement of altitude are initial radar offsets and refraction corrections. Since data from the three radar sites are usually available for most X-15 flights, the altitude uncertainty is reduced by carefully combining the three sets of data. The uncertainty does not exceed about ±1000 feet for ground distances greater than about 100 miles from Edwards. Less than 100 miles from Edwards, the altitude errors are ±500 feet and less.

Mach number determination is dependent on four measurements: radar velocity, and altitude, ambient temperature, and atmospheric winds. Coordinated analysis of radar data has placed radar-velocity errors (including winds) between 50 ft/sec and 75 ft/sec (ref. 24). These errors apply to Mach numbers greater than 1 and altitudes up to about 200,000 feet. Above this altitude, the effects of winds could result in velocity errors of 150 ft/sec or greater, because of uncertainty in the magnitude and direction of the winds. For example, figure 16(a) (adapted from ref. 26) illustrates the 2σ standard deviation (ref. 27) variability of the winds up to about 200,000 feet.

The standard-deviation error in rawinsonde temperature measurements is near 1° C up to approximately 50,000 feet (ref. 28). Between 50,000 feet and 100,000 feet, the standard-deviation temperature errors are within 1.5° C to 2.0° C (ref. 29). ARCAS bead thermistor temperature-measurement errors above 100,000 feet increase to 5° C at 150,000 feet (ref. 10). Errors in temperature measurements increase rapidly above 200,000 feet as a result of transition changes from continuum flow to slip flow over the thermistor (ref. 30).

For most X-15 flights, temperature sounding measurements above 150,000 feet have been questionable. Standard atmospheres (refs. 8 and 9) have been used to calculate the speeds of sound for Mach number determination above 150,000 feet. Figure 16(b) illustrates the deviation in temperatures from the U.S. Standard Atmosphere, 1962.

The standard deviation in rawinsonde ambient-pressure measurements for altitudes below 50,000 feet is ±3 millibars (±6.3 lb/ft^2) and ±1.5 millibars (±3.1 lb/ft^2) between 50,000 feet and 100,000 feet (ref. 31). Above 100,000 feet, ambient pressure was obtained from the U.S. Standard Atmosphere, 1962. The errors in ambient pressure are similar to errors in density that are shown in figure 16(c) (ref. 32).

Figure 17 shows the X-15 Mach number error that was estimated after assuming a standard deviation (1σ) of 50 ft/sec in radar velocity. Also, 1σ errors were assumed for winds and temperature. The figure shows that a 1σ Mach number error of ±0.05 would be representative for X-15 flights up to a Mach number of 6 and an altitude of 100,000 feet. Figure 17 also shows that for X-15 flight conditions up to an altitude of 200,000 feet the maximum Mach number of ±0.1 would correspond to a 2σ Mach number error.

Nose-Boom Pitot-Static Tube

The position-error calibration of the pitot-static tube mounted on the X-15 nose boom is discussed in reference 24. Magnitudes of errors in Mach number and altitude for the nose-boom pitot-static tube system and the ball-nose fuselage static system, which is discussed in the next section, are shown in figure 18. Mach number and pressure-altitude errors are primarily the result of position error and increase with Mach number. At M = 3.31, the highest Mach number attained with the nose-boom installation (ref. 33), the absolute errors were 0.18 in Mach number and 2200 feet in pressure altitude. The maximum altitude achieved by the X-15 with the nose-boom installation was 136,500 feet (ref. 34). The nose-boom pitot-static-tube error for both Mach number and altitude was insensitive to angles of attack up to approximately 12°, the maximum experienced.

12

Hypersonic Flow-Direction and Fuselage Static System

Mach number and altitude. — Use of the hypersonic flow-direction system and fuselage static system both separately and in combination has provided a source of varied air-data information. In contrast to the insensitivity exhibited by the nose-boom pitot-static tube, the altitude error due to the fuselage statics was very sensitive to angle of attack above $M = 1$ (fig. 18). Both Mach number and altitude errors increased with Mach number and decreased with increasing angle of attack. These errors are primarily induced by the position error of the fuselage static system. At $M = 3.31$, the maximum Mach number reached by the X-15 with the pitot-static tube, the errors in Mach number and altitude from the fuselage static system were, respectively, 0.88 and 12,400 feet for $\alpha = 0°$, and 0.50 and 6300 feet for $\alpha = 12°$.

Dynamic pressure. — Errors in determining dynamic pressure depend greatly on the altitude of the X-15. On the high-altitude flight depicted in figure 19(a), the X-15 reached dynamic pressures of less than 1 lb/ft^2; whereas, on the low-altitude flight, dynamic pressures of nearly 2000 lb/ft^2 were encountered. For both of the profiles dynamic-pressure errors were analyzed by using equations (3) and (4).

Measurement uncertainties used to determine dynamic-pressure errors were 0.1 in radar Mach number, 6 lb/ft^2 in ambient pressure (combination of radar altitude and rawinsonde errors), and ± 8.5 lb/ft^2 in stagnation pressure. The latter error was due to the recorder. A dynamic-pressure error of 5 percent results from the use of equation (3) for altitudes below 100,000 feet and Mach numbers between 1 and 6 (fig. 19(b), solid line). When equation (4) is used to determine dynamic pressure, errors indicated by the dashed lines in figure 19(b) are representative. For low-altitude flights, the dynamic-pressure error decreases rapidly from about 9 percent near a Mach number of 1 to about 2 percent at a Mach number of 2. The error further decreases rapidly to less than 1 percent at hypersonic Mach numbers. The errors in dynamic-pressure determination for high-altitude flights increase in the hypersonic Mach number range because of the low pressure level.

The increased accuracy in dynamic pressure obtained by the use of equation (4), with the ball-nose stagnation pressure, has made this the primary measurement method. This technique is used with the constraints that Mach numbers be larger than 2 and altitudes be 100,000 feet or less. For flight conditions beyond these limits, dynamic pressures are determined from the ball nose and radar measurement and are compared. The most accurate value of dynamic pressures is selected after analyzing both sets of data.

Pilot's q-Meter

To obtain a relationship for calibrating the q-meter, which is used by the pilot to determine real-time dynamic pressure, the factor $\left(1 - \dfrac{1}{7M^2}\right)^{2.5}$ in equation (4) was assumed to be 1 for Mach numbers greater than 2. The resulting relationship takes the form $q_p' \approx K p_{t_2}$ where q_p' is the indicated dynamic pressure and is a function of stagnation pressure alone. Two values of K (0.540 and 0.526) were analyzed

in order to provide the most accurate q'_p to the pilot. Figure 20(a) shows the theoretical errors in dynamic pressure obtained by selecting values for $\frac{q'_p}{p_{t_2}}$ of 0.526 and 0.540. The relationship $q'_p = 0.526p_{t_2}$ was selected for calibrating the pilot's q-meter because it gave a lower overall error over the Mach number range. For $K = 0.526$, the dynamic pressure indicated on the pilot's q-meter is 5 percent high at $M = 2.1$, and 2.5 percent low at $M = 6$.

Figure 20(b) shows the q-meter dynamic pressure for an entire X-15 flight. The error in the q-meter dynamic pressure increases rapidly as the Mach number decreases below 2. Indicated dynamic pressure obtained from cockpit film agrees to within 1 to 2 percent of the final reduced value of dynamic pressure for Mach numbers greater than 2.

Fuselage Pitot Probe

The ratio of the pitot-probe pressure p_{t_3} to the ball-nose stagnation pressure p_{t_2} is shown in figure 21 as a function of angle of attack and Mach number. For supersonic speeds below $M = 1.8$ and at subsonic speeds for which the probe was designed, no significant angle-of-attack or Mach number effects are noted. At supersonic speeds above $M \approx 1.8$, the pressure ratio is affected considerably by angle of attack and Mach number. For low angles of attack ($0° \leq \alpha \leq 5°$), p_{t_3} is higher than p_{t_2}; whereas, for the higher angles of attack ($10° \leq \alpha \leq 15°$), p_{t_3} is less than p_{t_2}.

Stagnation-Temperature Probe

The temperature probe was flown to a Mach number of 6 and altitudes above 250,000 feet. Factors leading to velocity errors based on the temperature-probe measurements are: recovery-factor uncertainty, calibration uncertainty, radiation effects, and the assumption that ambient enthalpy H is a constant. Figure 22 shows velocity errors derived from errors in stagnation-temperature measurements plotted against dynamic pressure. All the data are for Mach numbers from 2 to 6. For dynamic pressures from 200 lb/ft^2 to 1000 lb/ft^2, the velocity obtained from the temperature probe was, on an average, 3 percent higher than faired radar velocities. As dynamic pressure decreased below 100 lb/ft^2, the velocity errors increased rapidly. For X-15 flights above 100,000 feet, the convective heat transfer to the probe's elements is reduced by the lower-density airflow through and around the probe. As a result the radiation heat loss and velocity errors are large. A hysteresis effect is shown in figure 22 by the larger velocity errors during atmospheric reentry than during atmospheric exit.

Inertial System

Figure 23(a) illustrates the altitude errors of the inertial flight data system for several high-altitude flights. The divergence from radar altitude became noticeable or objectionable only during the last half of each flight, after peak velocity and altitude

had been attained. The inertial-system performance is such that the altitude errors are about 5000 feet or less for the first 300 seconds after launch. Figure 23(b) compares radar and inertial velocities for an X-15 high-altitude flight. Both velocities are ground referenced. The inertial velocity differed from the radar velocity by no more than about 70 ft/sec for this and most other flights.

ANALYSIS OF AIR-DATA PARAMETERS FOR X-15 TIME HISTORY

For each X-15 flight, a complete flight time history is obtained by utilizing the radar-tracking data in conjunction with various onboard sensors. During the X-15 flight program, every onboard sensor has been used advantageously to supplement or fill in segments of missing radar data. It should be noted that the procedure is followed for both high-altitude and low-altitude flights and, in any given flight, different sensors are used at different times.

Time Correlation and Peak Velocity

For X-15 flights radar data are obtained in time-of-day format, whereas onboard data are obtained in internal-event format. To analyze both sets of data, comparison on a basis of common time is essential. This is accomplished by telemetering several onboard parameters to the Edwards control room. The time correlation is made to within 1/10 second by utilizing the sharp "jump" in the telemetered normal-accelerometer trace at launch.

Peak velocity is determined by utilizing onboard accelerations at the center of gravity of the X-15 airplane to supplement radar data. Radar data must be supplemented because of their low response rate to space-position changes and the fact that the data-reduction smoothing process rounds off peak velocity. Figures 24(a) and 24(b) show the altitude profile and corresponding airplane normal and longitudinal accelerations as a function of time for the complete flight. To help establish the peak velocity, longitudinal acceleration is integrated with respect to time for a short time segment near the approximate burnout point. Figure 24(c) shows the integrated longitudinal acceleration along with radar data plotted to an enlarged time scale near the approximate burnout point. Peak velocity and burnout occur at the abrupt change in slope of the integrated velocity. For most X-15 flights, peak velocity occurs earlier than would be indicated by radar velocity.

Time History of a Complete Flight

Figures 25 and 26 compare the final values of onboard air-data parameters with radar-calculated values for an altitude flight. Figure 25 shows the faired values of altitude and dynamic pressure, and figure 26 shows velocity and calculated Mach number.

Since the X-15 is launched at a Mach number of about 0.8, the position error is small enough for the internally recorded pressure to be used for altitude determination. However, as Mach number increases from $M \approx 0.8$ to $M \approx 1.0$, the indicated altitude will be, respectively, from about 500 feet to about 1000 feet lower than the true value. The corrected pressure altitude at launch is used to determine the most reliable

radar-altitude data source for this flight phase. For the example flight selected, the Beatty radar data at launch agreed with the corrected internal-pressure altitude and was selected as the most accurate altitude source.

As the X-15 reached higher altitudes, the accuracy of measurement of elevation tracking angle improved; hence, the altitude measurements improved for both the Ely and Edwards radars. The Ely radar altitude agreed with the Beatty radar starting at 55,000 feet, while Edwards radar altitude merged with Beatty near 85,000 feet. As the tracking range increased from the launch point, both Beatty and Ely radar data became less accurate and more reliance was placed on Edwards data. From the data, it can be seen that the internally recorded pressure (fuselage static) altitude was, as expected, low when the airplane reached transonic speeds in the landing approach. Initially, the recorded pressure altitude was 1000 feet lower than the true value, but then merged with the Edwards radar altitude below $M = 0.9$. Figure 26 shows that the radar velocities calculated from the radar sources follow the same trends as the altitudes. The inertial velocity was within 70 ft/sec of the faired radar velocity over most of the flight. The inertial-platform altitude was 1000 feet low at launch and about 5000 feet high after 300 seconds.

The stagnation-temperature-probe velocity corresponded well with the faired radar velocities until the flight region was reached where dynamic pressure became low (less than 100 lb/ft^2). The stagnation-temperature-probe velocity was then as much as 1600 ft/sec lower than the faired radar velocities. When higher dynamic pressure was encountered during reentry, the probe's velocity merged with the faired radar velocity.

Faired radar altitude and velocity were used to calculate dynamic pressure, using equation (3), and then compared to ball-nose-determined dynamic pressure by using equation (4). Except near $M = 1$ and for dynamic pressures below 100 lb/ft^2, the differences were 1 to 2 percent. The relationship $p = \dfrac{q}{0.7M^2}$, with q obtained from equation (4) and Mach number obtained from faired radar and rawinsonde data, has been used to calculate X-15 altitudes. The calculated altitudes have agreed with the radar-faired altitudes to within ±1000 feet or better on all flights. This method provides another means of selecting the correct radar-altitude tracking data.

For X-15 flights to about 100,000 feet and less, the same procedures as those just described are generally used for altitude and velocity determination. For high Mach number, low altitude flights, dynamic pressure is of prime importance; thus, q calculated from the ball-nose stagnation pressure is utilized above a Mach number of 2.

Useful Flight Regions for the Onboard Sensors

Figure 27 shows as a function of flight profile the areas in which several X-15 onboard guidance sensors can be used most reliably. A typical high-altitude flight profile is shown in figure 27(a), and a typical low-altitude profile is shown in figure 27(b). The length and location of the horizontal shaded bar, for a particular flight-guidance sensor, relative to the time portion of the flight profile, indicates where the sensor can be used reliably. For the low-altitude profile most of the sensors can be used for the entire flight. For the high-altitude profile, the horizontal shaded bars show breaks because of the measurement problems discussed.

16

Some of the flight sensors of the type used on the X-15, and their associated problems, will no doubt be encountered in future flight research programs. Several air-data measurement problems predicted for lifting reentry and glide vehicles (ref. 35) are similar to those already encountered with the X-15 airplane.

CONCLUDING REMARKS

The integration of data from several onboard sensors is needed for pilot use during X-15 flights and later for data analysis. During the X-15 program, procedures were developed for integrating flight-guidance sensor, meteorological balloon, rocketsonde, and radar data to provide reliable air-data parameters. The information thus gained can be used to extend the usefulness of the X-15 air-data sensors. A single onboard sensor that will provide reliable velocity and altitude data for flight conditions as varied as those encountered by the X-15 airplane is not available at this time. Advantages and disadvantages of the several onboard sensors used in the X-15 flight program are summarized in the following paragraphs.

The advantages of the nose-boom pitot-static tube were:

1. Small increasing position error with increasing Mach number, compared to fuselage static system.

2. Insensitive in indicated ambient-pressure readings for angles of attack from 0° to 12°.

3. Accurate measurement of stagnation pressure between angles of attack of -13° to 32°.

The disadvantages of the nose-boom pitot-static tube were:

1. A long, slender boom presented aerodynamic-heating problems at Mach numbers above about 3.

2. Ambient-pressure errors increased at angles of attack larger than 12°.

The advantages of the hypersonic flow-direction sensor and fuselage static system are:

1. Stagnation pressure can be sensed accurately over large angle-of-attack (-20° to 40°) and angle-of-sideslip (±20°) ranges.

2. High temperatures at Mach numbers greater than 3 can be withstood.

The disadvantages of the hypersonic flow-direction sensor and fuselage static system are:

1. Large position error and sensitivity to variations in angles of attack for Mach numbers greater than 1, primarily because of use of fuselage static orifices, make altitude and Mach number difficult to measure.

2. Risk of servosystem failure during flight.

17

The advantages of the fuselage pitot probe are:

1. Contains no electronics that might fail during flight.

2. Provides accurate stagnation pressures below a Mach number of 1.8 for landing information.

The disadvantages of the fuselage pitot probe are:

1. Rapidly increasing position error above a Mach number of 1.8.

2. Large sensitivity to angle-of-attack variations for Mach numbers above 1.8.

The advantages of the stagnation-temperature probe are:

1. Can provide a direct indication of free-stream velocity to the pilot.

2. Provides a system for free-stream velocity independent of pressure-sensing system.

3. For dynamic pressures between 100 lb/ft^2 and 1000 lb/ft^2 and velocities up to 6000 ft/sec, the velocity derived from the temperature probe differed by 3 percent on the average from radar velocity.

The disadvantages of the stagnation-temperature probe are:

1. Radiation errors became excessive for dynamic pressures below 100 lb/ft^2.

2. Recovery-factor determination and temperature-probe calibration present problems.

The advantages of the inertial flight data system are:

1. Inertial guidance system is self-contained and independent of the flight environment.

2. The X-15 pilot is presented with satisfactory inertial altitude, velocity, and rate of climb during the first 300 seconds of flight.

The disadvantages of the inertial flight data system are:

1. System is complex and subject to malfunction.

2. Inertial-altitude error is unbounded and increases exponentially with time, becoming larger than 5000 feet after 300 seconds of X-15 flight.

3. Inertial data errors are contained in the data output for the entire flight.

Flight Research Center,
    National Aeronautics and Space Administration,
        Edwards, Calif., November 21, 1967,
            126-16-06-03-24.

18

APPENDIX A

SUMMARY OF X-15 RADAR DATA-REDUCTION PROCESS

The range, azimuth, and elevation are obtained in binary count every 1/10 second. The radar data-reduction program for the IBM 7094 computer consists of six separate decks: read, smooth, calculation, transformation, velocity, and print.

The read deck reads the control cards and uses the information to read the data tape written by the ground station. First, the proper file is positioned, then the start time is found. The frame is examined to determine if the format is correct. Next, the first differences between this point and the last point are computed and checked to ascertain if magnitudes of the differences are possible. If the point is not possible, the possibility of bit dropout is examined. Otherwise, the point is considered a "wild" point and is corrected. A point is determined to be "wild" by the following method: A quadratic curve is fitted by the method of least squares to six points. The six points consist of the three immediately preceding and the three immediately following the point under consideration. A point is considered to be "wild" if it does not lie within three standard deviations of the fitted curve. Wild points are replaced by the corresponding point that lies on the curve.

Next, the smooth deck reads the tape written by the read deck. First, it searches for the time of the data point desired, as determined by the start time and sample rate. For the starting time, the program uses the 15 preceding points and the 15 following points. Then, a least-square weighed polynomial curve fit of the seventh degree is made over seven points at a time. The smoothing of the data is repeated two times after the initial pass. When a point is considered questionable in the smoothing operation, a quadratic is fitted through the point and six other points. If the point in question is considered to be incorrect, it is replaced by the corresponding point on the curve.

The calculation deck corrects for radar-antenna offset and converts the data in counts into feet and radians. Next, the data are corrected for refraction effects (appendix B) and converted from spherical to X, Y, and Z rectangular coordinates. The position of a vehicle as acquired by the Edwards, Beatty, and Ely radar sites is computed in rectilinear coordinate system as given by the following sketch in which

$$X_{2k} = R \cos E \sin A \text{ (positive east)}$$

$$Y_{2k} = R \cos E \cos A \text{ (positive north)}$$

$$Z_{2k} = R \sin E \text{ (positive vertical)}$$
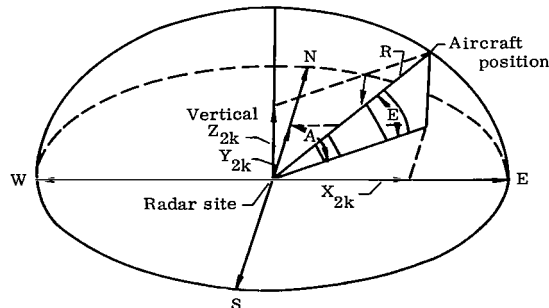
The X_{2k} and Y_{2k} position components are oriented in a plane tangent to the earth at the feed point of the radar dish at each site. The radar obtaining the position data is designated as the local origin of the coordinate system, and the data are to be transferred (transformation deck) to the principal origin, Edwards. The following equations indicate the aircraft's position in relation to a circular arc on the surface of the earth intercepting the Edwards and Ely radar sites (High Range):

$$X_r = X_{2k} \cos \theta_1 - Y_{2k} \sin \theta_1$$

$$Y_r = X_{2k} \sin \theta_1 + Y_{2k} \cos \theta_1$$

$$Z_r = Z_{2k}$$

The following sketch indicates the relationship of the radar sites and the angles used in the equations:
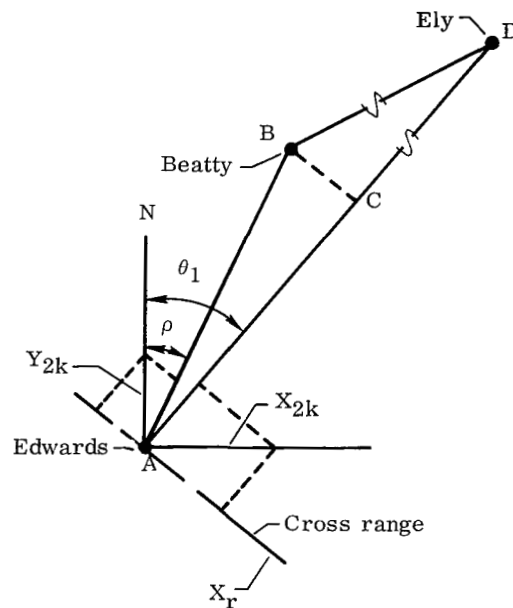
where

$$\theta_1 = 26°23'27.70''$$

$$\rho = 21°51'29.87''$$

$$AB = 279,321.80 \text{ yd}$$

$$BD = 317,131.83 \text{ yd}$$

$$DC = 316,385.03 \text{ yd}$$

$$CA = 278,467.33 \text{ yd}$$

The following sketch is a projection of the radar range and elevation on a plane passing through the center of the earth along the High Range centerline. Cross range is, therefore, perpendicular to the plane of the paper.
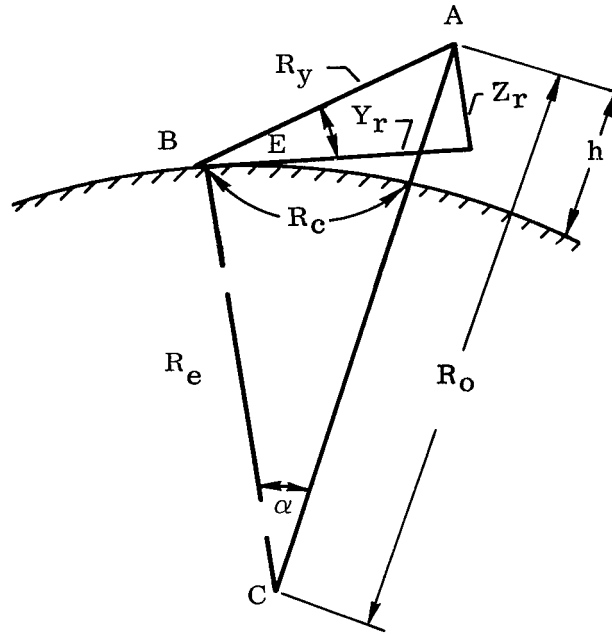
The ground range R_c is then computed from the following relation:

$$R_y = \sqrt{Y_r^2 + Z_r^2}$$

From the preceding sketch and using the law of cosines, the relationship for R_o is

$$R_o = \sqrt{R_e^2 + R_y^2 + 2R_e Z_r}$$

and the central angle is approximately

$$\alpha \approx \sin^{-1} \frac{Y_r}{R_o}$$

and

$$R_c = R_e \alpha$$

The altitude of the aircraft above mean sea level is given by the approximation

$$h \approx \sqrt{R_e^2 + R_y^2 + 2R_e Z_r} - R_e + h_o$$

where

$$R_e = \text{mean radius of the earth} = 20,887,130 \text{ ft}$$

$$h_o = \text{tracking-station altitude above mean sea level}$$

The basic reference data used in the program were as follows:

Station	Latitude	Longitude	h_o, ft
Edwards	34°56'59.311"	117°53'11.524"	2339.67
Beatty	37°04'54.036"	116°49'09.030"	4964.30
Ely	39°18'31.047"	115°05'08.299"	9257.70

The velocity deck determines the velocity components of the aircraft. Since all runs are less than 1500 points, the data are differentiated for the entire run during one pass.

The print deck performs the following main functions: The rawinsonde weather data for the event are supplemented in the deck by the U.S. Standard Atmosphere, 1962. The velocity components are corrected for winds, assuming the wind data obtained from the rawinsonde balloon launched from Edwards are constant over the test range.

APPENDIX B

REFRACTION CORRECTIONS

The elevation-angle correction is based upon simple surface-level observations of atmospheric properties at the radar site. A stratified atmosphere is normally assumed to exist within the range of any particular radar. Since only limited atmospheric data are available at the Beatty and Ely sites, a model atmosphere constructed for Edwards is used to correct data taken at the other sites.

The surface index of refraction at each radar site is computed from the relationship (from ref. 1)

$$n = \frac{R_O}{10^6} + 1$$

where

n = index of refraction of the form 1.000XXX

R_O = contribution due to water-vapor pressure

R_O and S are calculated as follows (from ref. 1):

$$R_O = \frac{2.26}{T^2_{(°K)}} e^\lambda$$

where

$$\lambda = \left[(.5369) \left(\frac{1}{273} - \frac{1}{T_{dl}} \right) \right]$$

$$S = \frac{77 p_{mb}}{T^2_{(°K)}}$$

where

S = contribution due to pressure and temperature

$T_{(°K)}$ = surface temperature in degrees Kelvin

T_{dl} = surface dew point in degrees Kelvin

p_{mb} = surface pressure in millibars

A more convenient form of index of refraction was found by defining an N unit, designated by N, where

$$N = (n - 1) \times 10^6$$

The functions used to correct the elevation angle for each data point are defined as

$$\Delta E = \frac{K_{1E} D}{K_{2E} + Z}$$

where

$$D \approx R \cos E \text{ (ground range)}$$

$$Z = R \sin E \text{ (altitude above a plane)}$$

and

$$R = \text{radar slant range in yards}$$

$$E = \text{radar elevation angle}$$

K_{1E} is the above-mentioned surface N unit $\times 10^{-3}$ converted to Army mils, as follows:

$$K_{1E} = K_{am} N \times 10^{-3}$$

where

$$K_{am} = 1.01859 \text{ mils}$$

K_{2E} has been computed in the following table from atmospheric conditions at Edwards:

K_{1E}	K_{2E}	K_{1E}	K_{2E}	K_{1E}	K_{2E}
0.2241	21,410.6	0.2669	17,296.8	0.3076	14,803.3
.2261	21,160.5	.2689	17,147.1	.3097	14,701.2
.2281	20,916.6	.2709	17,000.6	.3117	14,600.9
.2302	20,679.8	.2730	16,857.2	.3137	14,502.2
.2322	20,449.3	.2750	16,716.7	.3158	14,405.1
.2343	20,224.7	.2771	16,579.0	.3178	14,309.7
.2363	20,005.9	.2791	16,444.2	.3198	14,215.7
.2384	19,792.9	.2811	16,312.0	.3219	14,123.3
.2404	19,585.2	.2832	16,182.2	.3239	14,032.4
.2424	19,382.8	.2852	16,055.2	.3259	13,942.8
.2445	19,185.4	.2872	15,930.4	.3280	13,854.7
.2465	18,993.0	.2893	15,808.2	.3300	13,767.9
.2485	18,804.8	.2913	15,688.1	.3321	13,682.5
.2506	18,621.5	.2934	15,570.5	.3341	13,598.3
.2526	18,442.3	.2954	15,454.9	.3361	13,515.4
.2546	18,267.3	.2974	15,341.4	.3382	13,433.8
.2567	18,096.4	.2995	15,229.9	.3402	13,533.2
.2587	17,929.1	.3015	15,120.4	.3422	13,274.0
.2608	17,765.9	.3035	15,012.8	.3443	13,195.8
.2628	17,606.1	.3056	14,907.2	.3463	13,118.8
.2648	17,449.7				

The equation for elevation-angle correction after correction to radians becomes

$$\Delta E_{rad} = \frac{\Delta E K_{mr}}{10^3}$$

where

$$K_{mr} = 0.981747 \text{ milliradians}$$

The corrected elevation angle is now found from

$$E_c = E - \Delta E_{rad}$$

REFERENCES

1. Pearson, Kermit E.; Kasparek, Dennis D.; and Tarrant, Lucile N.: The Refraction Correction Developed for the AN/FPS-16 Radar at White Sands Missile Range. Tech. Memo. 577, U.S. Army Signal Missile Support Agency, Nov. 1958.

2. Anon.: Radiosondes AN/AMT-4A and AN/AMT-4B. TM 11-2432A to 31M4-2AMT4-11, Depts. of the Army and the Air Force, June 1958. (Supersedes TM 11-2432A.)

3. Anon.: Manual of Radiosonde Observations (WBAN). Circular P, Seventh Edition. U.S. Weather Bur., U.S. Air Force, U.S. Navy, June 1957.

4. Daniel, O. H.: Electronic Computer Reduction of Upper Air Data. 4WG Pamphlet No. 105-7-2, 4th Weather Group, Air Weather Service (MATS), U.S. Air Force, June 1961.

5. Appleman, H. S.: A Preliminary Analysis of Mean Winds to 220,000 Feet. Tech. Rep. 173, Air Weather Service (MATS), U.S. Air Force, Oct. 1963.

6. Massey, H. S. W.; and Boyd, R. L. F.: The Upper Atmosphere. Hutchinson & Co. (London), 1960.

7. Wagner, N. K.: Theoretical Accuracy of the Meteorological Rocketsonde Thermistor. Rep. No. 7-23, U.S. Army Electronics Research and Development Activity (White Sands Missile Range, N. Mex.), July 1, 1963.

8. Minzner, R. A.; Ripley, W. S.; and Condron, T. P.: U.S. Extension to the ICAO Standard Atmosphere. Tables and Data to 300 Standard Geopotential Kilometers. Geophysics Res. Directorate and U.S. Weather Bur., 1958.

9. Anon.: U.S. Standard Atmosphere, 1962. NASA, U.S. Air Force, U.S. Weather Bur., Dec. 1962.

10. Stroud, W. G.; and Nordberg, William: Seasonal, Latitudinal and Diurnal Variations in the Upper Atmosphere. NASA TN D-703, 1961.

11. Sissenwine, Norman: Demarcation Between Upper Atmosphere and Space. Research Bulletin, Air Force Cambridge Research Laboratories (Hanscom Field, Mass.), Nov. 1963, p. 6.

12. Richardson, Norman R,; and Pearson, Albin O.: Wind-Tunnel Calibrations of a Combined Pitot-Static Tube, Vane-Type Flow-Direction Transmitter, and Stagnation-Temperature Element at Mach Numbers From 0.60 to 2.87. NASA TN D-122, 1959.

13. Gracey, William: Wind-Tunnel Investigation of a Number of Total-Pressure Tubes at High Angles of Attack. Subsonic, Transonic, and Supersonic Speeds. NACA Rep. 1303, 1957. (Supersedes NACA TN 3641.)

14. Wolowicz, Chester H.; and Gossett, Terrence D.: Operational and Performance Characteristics of the X-15 Spherical, Hypersonic Flow-Direction Sensor. NASA TN D-3070, 1965.

15. Cary, John P.; and Keener, Earl R.: Flight Evaluation of the X-15 Ball-Nose Flow-Direction Sensor as an Air-Data System. NASA TN D-2923, 1965.

16. Larson, Terry J.; and Montoya, Earl J.: Stratosphere and Mesosphere Densities Measured With the X-15 Airplane. J. Geophys. Res., vol. 69, no. 24, Dec. 1964, pp. 5123-5130.

17. Larson, Terry J.; and Covington, M. Alan: A Technique for Measuring Mesospheric Densities With the X-15 Research Airplane. Paper No. 66-441, AIAA, June 1966.

18. Fischel, Jack; and Webb, Lannie D.: Flight-Informational Sensors, Display, and Space Control of the X-15 Airplane for Atmospheric and Near-Space Flight Missions. NASA TN D-2407, 1964.

19. Jakob, Max: Heat Transfer. Vol. II. John Wiley & Sons, Inc., 1959, p. 182.

20. Hansen, C. Frederick: Approximations for the Thermodynamic and Transport Properties of High-Temperature Air. NASA TR R-50, 1959. (Supersedes NACA TN 4150.)

21. Eckert, E. R. G.; and Drake, Robert M., Jr.: Heat and Mass Transfer. Second ed., McGraw-Hill Book Co., Inc., 1959, p. 265.

22. Pitman, George R., Jr.: Inertial Guidance. John Wiley & Sons, Inc., 1962, p. 37.

23. Parvin, Richard H.: Inertial Navigation - Principles of Guided Missile Design. D. Van Nostrand Co., Inc., 1962, p. 224.

24. Larson, Terry J.; and Webb, Lannie D.: Calibrations and Comparisons of Pressure-Type Airspeed-Altitude Systems of the X-15 Airplane From Subsonic to High Supersonic Speeds. NASA TN D-1724, 1963.

25. Belmont, A.; Peterson, R.; and Shen, W.: Evaluation of Meteorological Rocket Data. NASA CR-138, 1964, p. 11.

26. Kantor, A. J.; and Cole, A. E.: Zonal and Meridional Winds to 120 Kilometers. J. Geophys. Res., vol. 69, no. 24, Dec. 15, 1964, pp. 5131-5140.

27. Reddick, H. W.; and Miller, F. H.: Advanced Mathematics for Engineers. Third ed., John Wiley & Sons, Inc., 1955, pp. 379-381.

28. Anon.: Accuracies of Radiosonde Data. AWS Tech. Rep. 105-133, Military Air Transport Service, U.S. Air Force, Sept. 1955.

29. Anon.: Temperatures at the 10-mb (101,000-Foot) Level. AWS Tech. Rep. 105-108, Military Air Transport Service, U.S. Air Force, May 1953.

30. Schaaf, Samuel A.; and Chambré, Paul L.: Flow of Rarefied Gases. Princeton University Press, 1961, p. 5.

31. Ference, Michael, Jr.: Instruments and Techniques for Meteorological Measurements. Compendium of Meteorology, Thomas F. Malone, ed., American Meteorological Soc. (Boston, Mass.), 1951, pp. 1207-1222.

32. Cole, Allen E.; and Kantor, Arthur J.: Air Force Interim Supplemental Atmospheres to 90 Kilometers. Air Force Surveys in Geophysics No. 153 (AFCRL-63-936), Air Force Cambridge Res. Lab., Dec. 1963.

33. Stillwell, Wendell H.; and Larson, Terry J.: Measurement of the Maximum Speed Attained by the X-15 Airplane Powered With Interim Rocket Engines. NASA TN D-615, 1960.

34. Stillwell, Wendell H.; and Larson, Terry J.: Measurement of the Maximum Altitude Attained by the X-15 Airplane Powered With Interim Rocket Engines. NASA TN D-623, 1960.

35. Dommasch, Daniel O.: Summary of Requirements for Air Data Sensors on Lifting Re-Entry and Glide Return Systems. Tech. Doc. Rep. No. FDL-TDR-64-73, Air Force Flight Dynamics Lab. (Wright-Patterson Air Force Base), Aug. 1964.
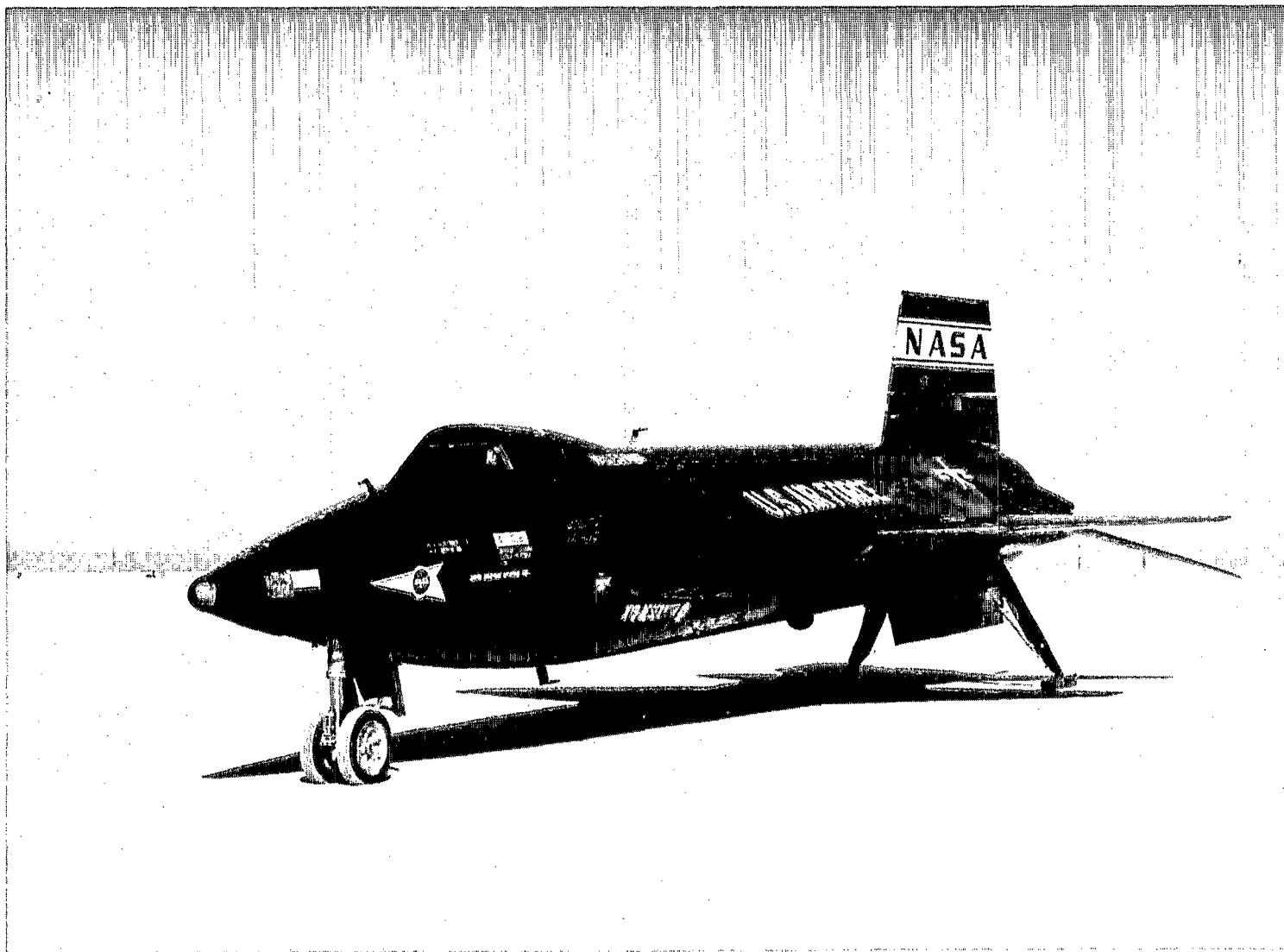
Figure 1.— X-15 airplane with ball nose.

E-7902
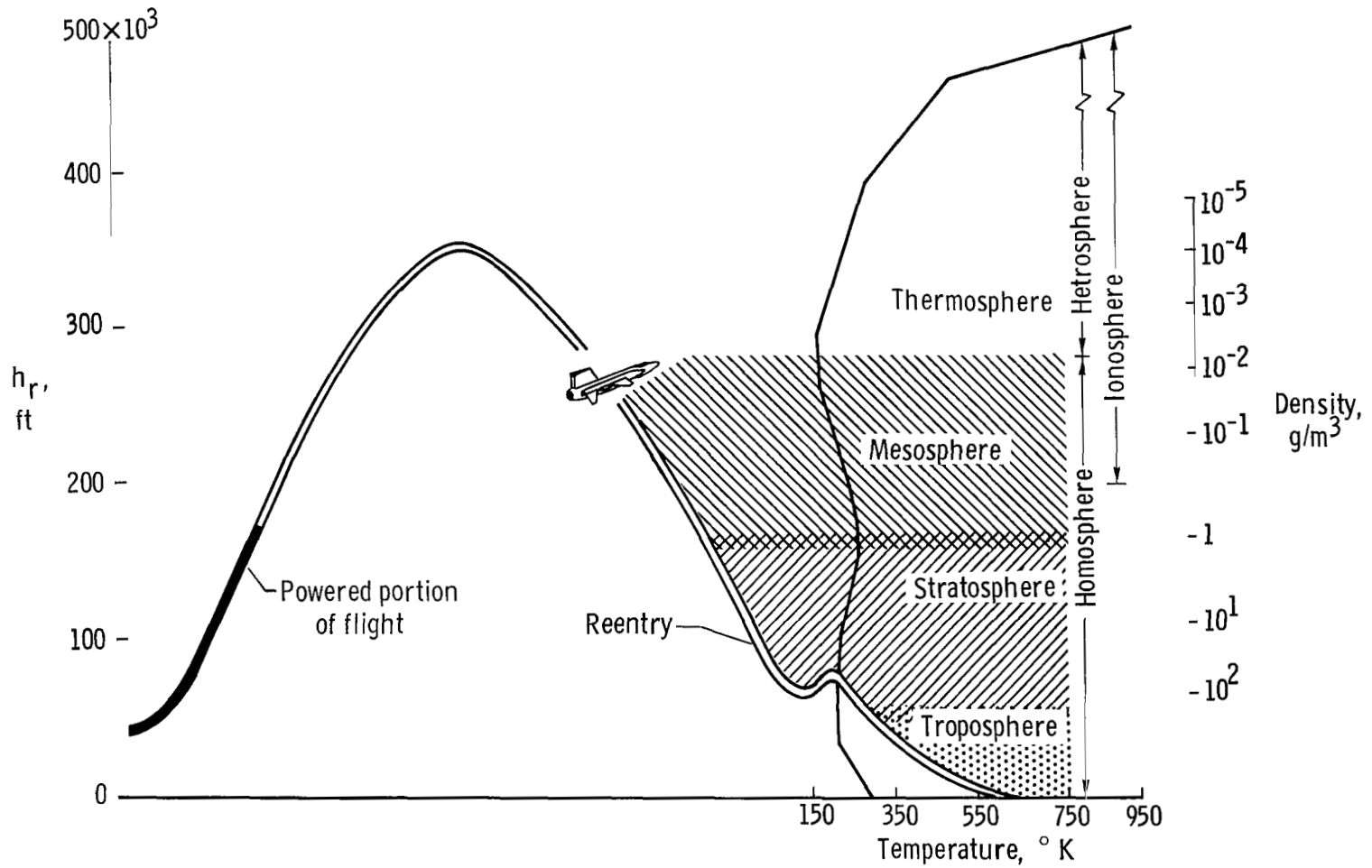
Figure 2.— Pictorial representation of the general X-15 flight performance capability and the atmospheric environmental conditions traversed.
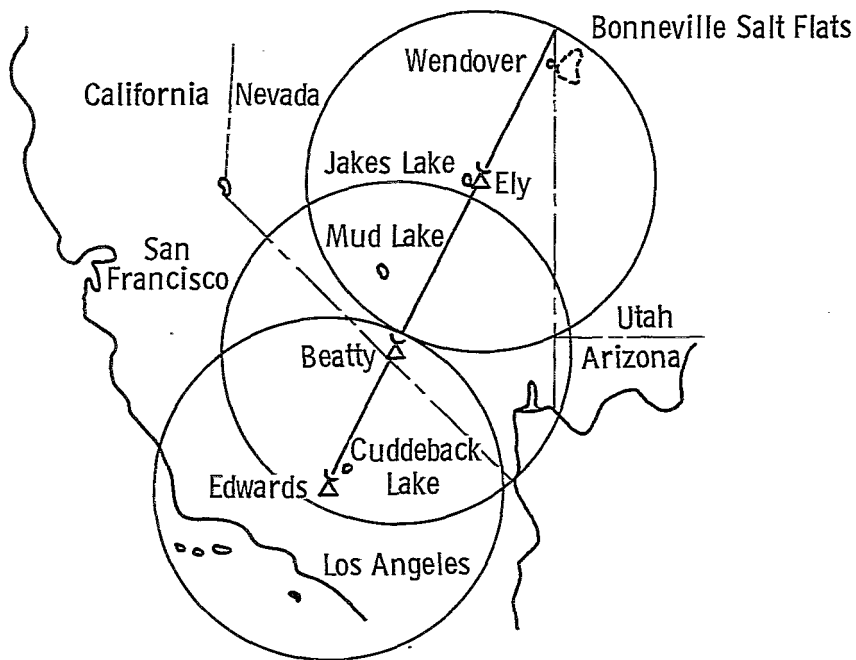
(a) High Range.
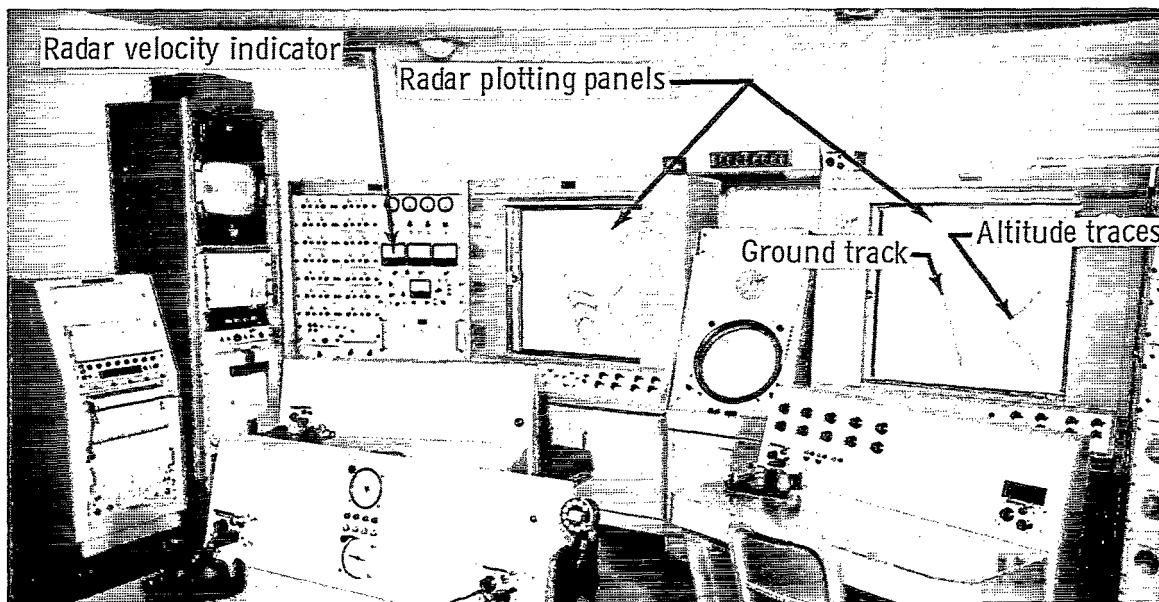
(b) Edwards ground control room.   E-9379

Figure 3. — Radar tracking range and Edwards ground control room.
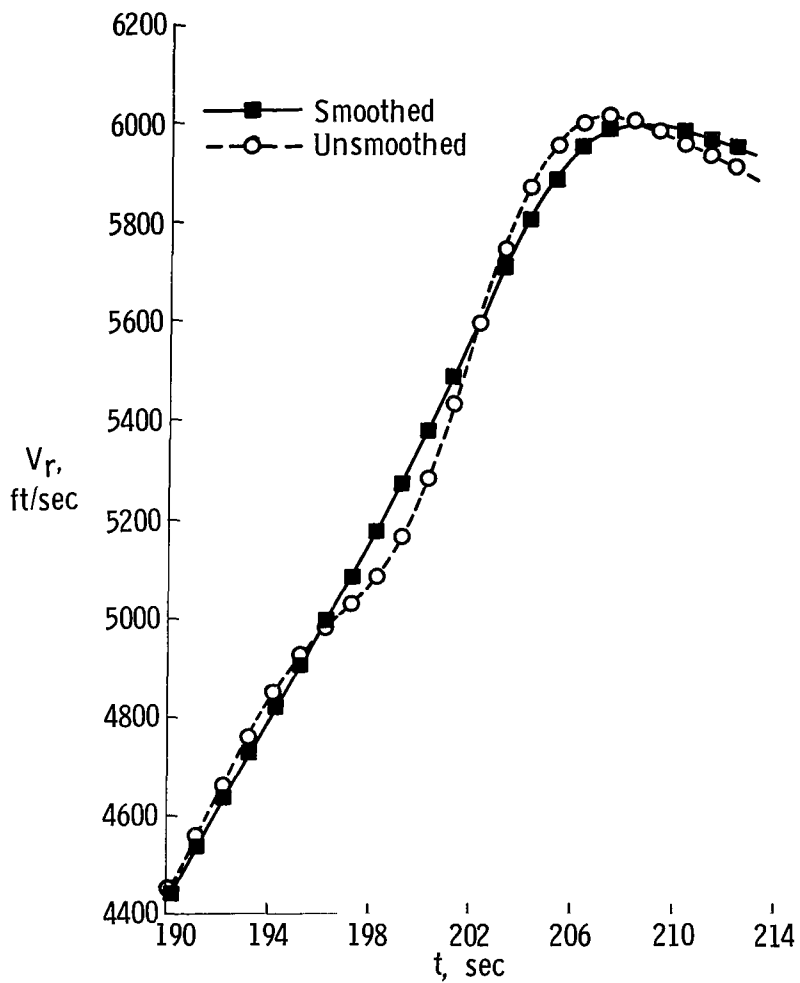
(a) Smoothed and unsmoothed radar velocity.
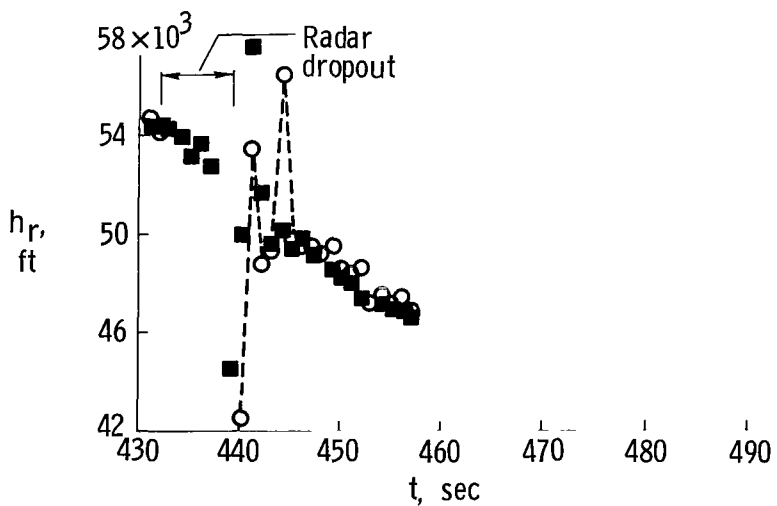
(b) Computer smoothing of a missing segment of data.

Figure 4.— Comparison of unsmoothed and smoothed radar velocity and altitude for two time increments of an X-15 flight.
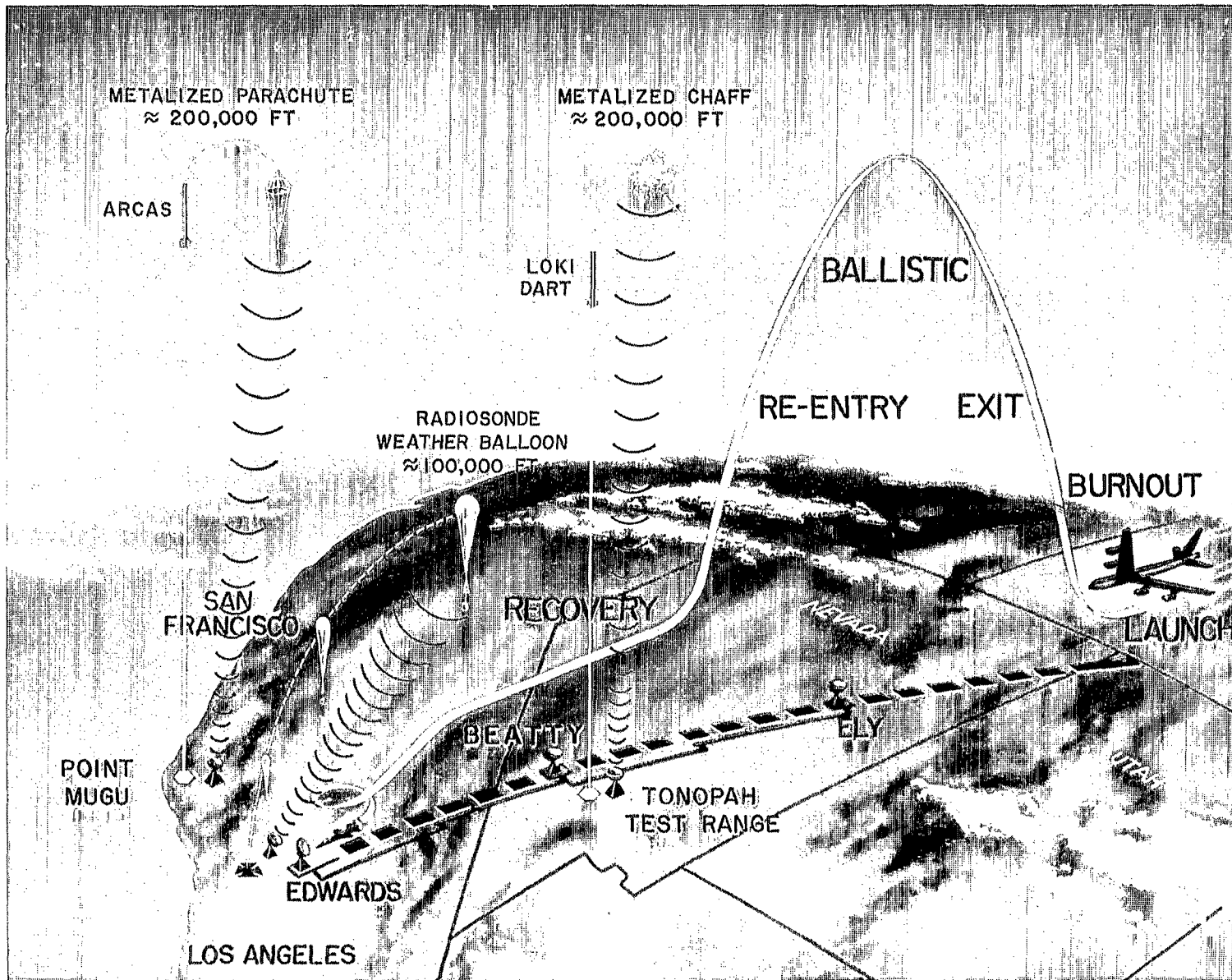
Figure 5.— Pictorial representation of an X-15 altitude mission and its relationship to meteorological sounding rockets fired to obtain atmospheric data.
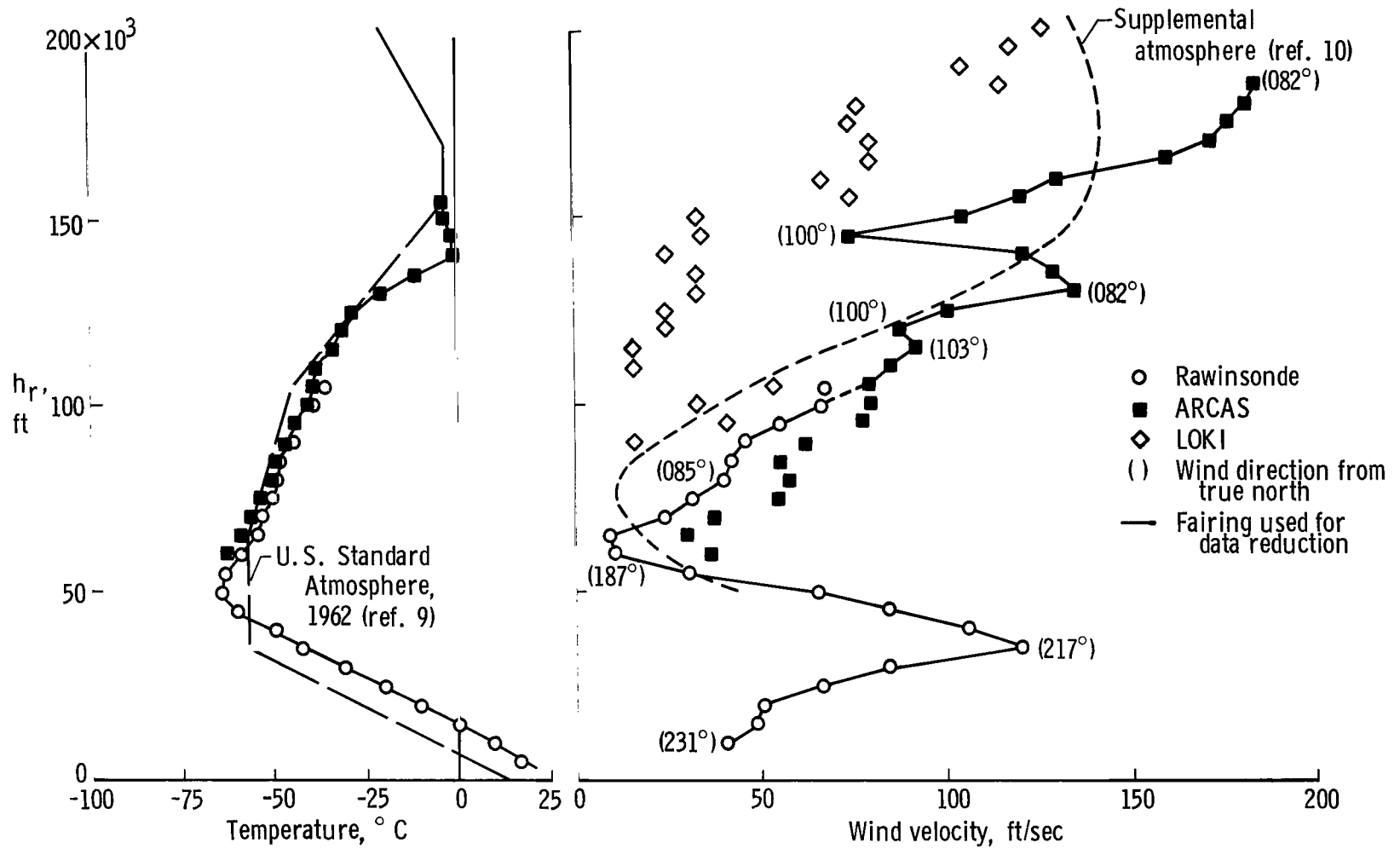
Figure 6.— Temperature and wind data obtained from several meteorological sources
for a typical X-15 high-altitude flight.

Total-pressure tube

Static orifices

Angle-of-attack vane

Angle-of-sideslip vane

1

0.015 wall

10°

Enlarged section of
pitot-static tube end

71

32 5/8

Upper surface

Angle-of-attack
vane

1 3/4

7.9

7/8

Static orifices

X-15 nose

27 1/4

Angle-of-sideslip
vane

8 3/4
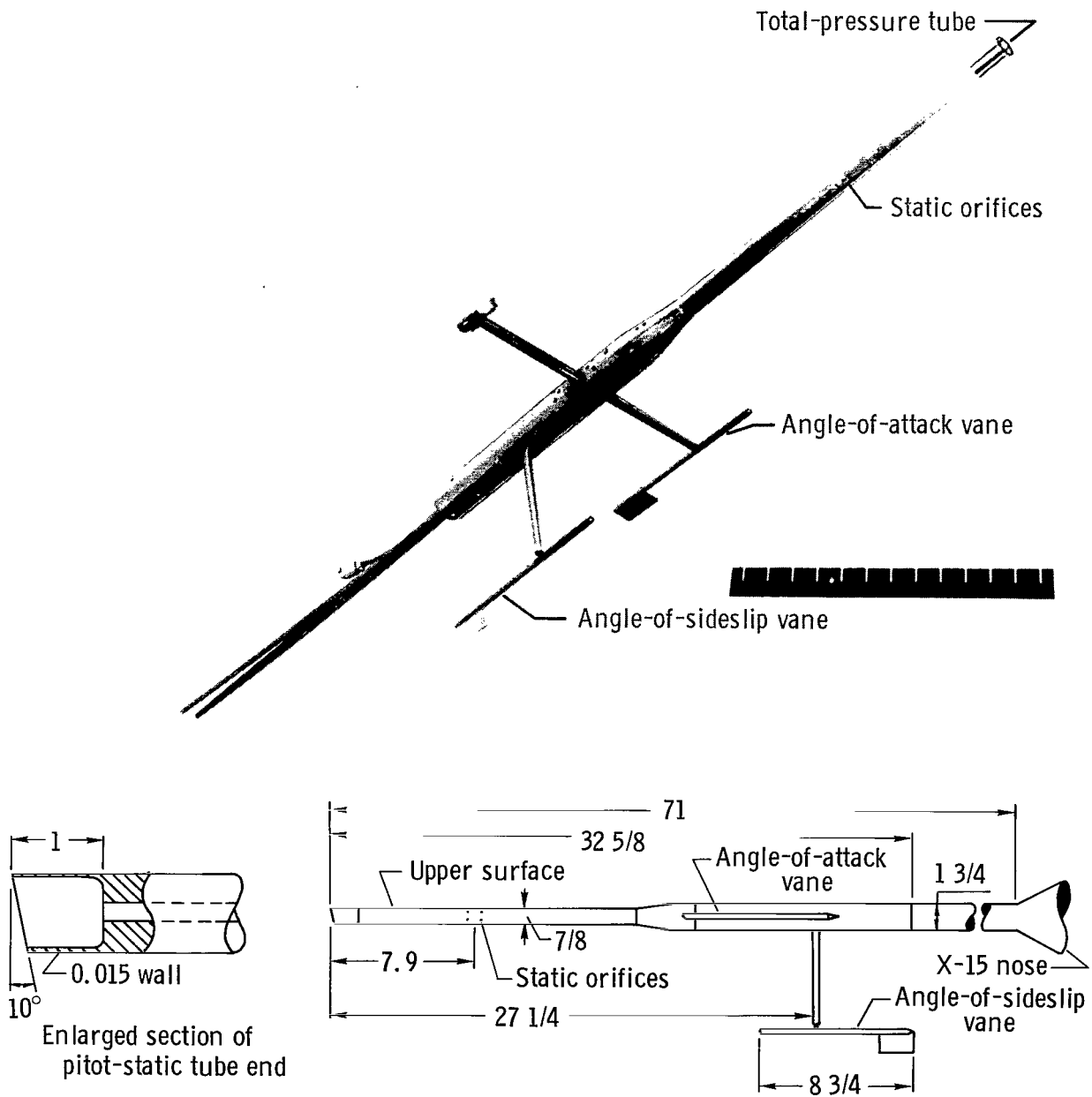
Figure 7.— Photograph and schematic drawing of the X-15 nose-boom
pitot-static tube with flow-direction vanes. Dimensions
in inches unless otherwise noted.
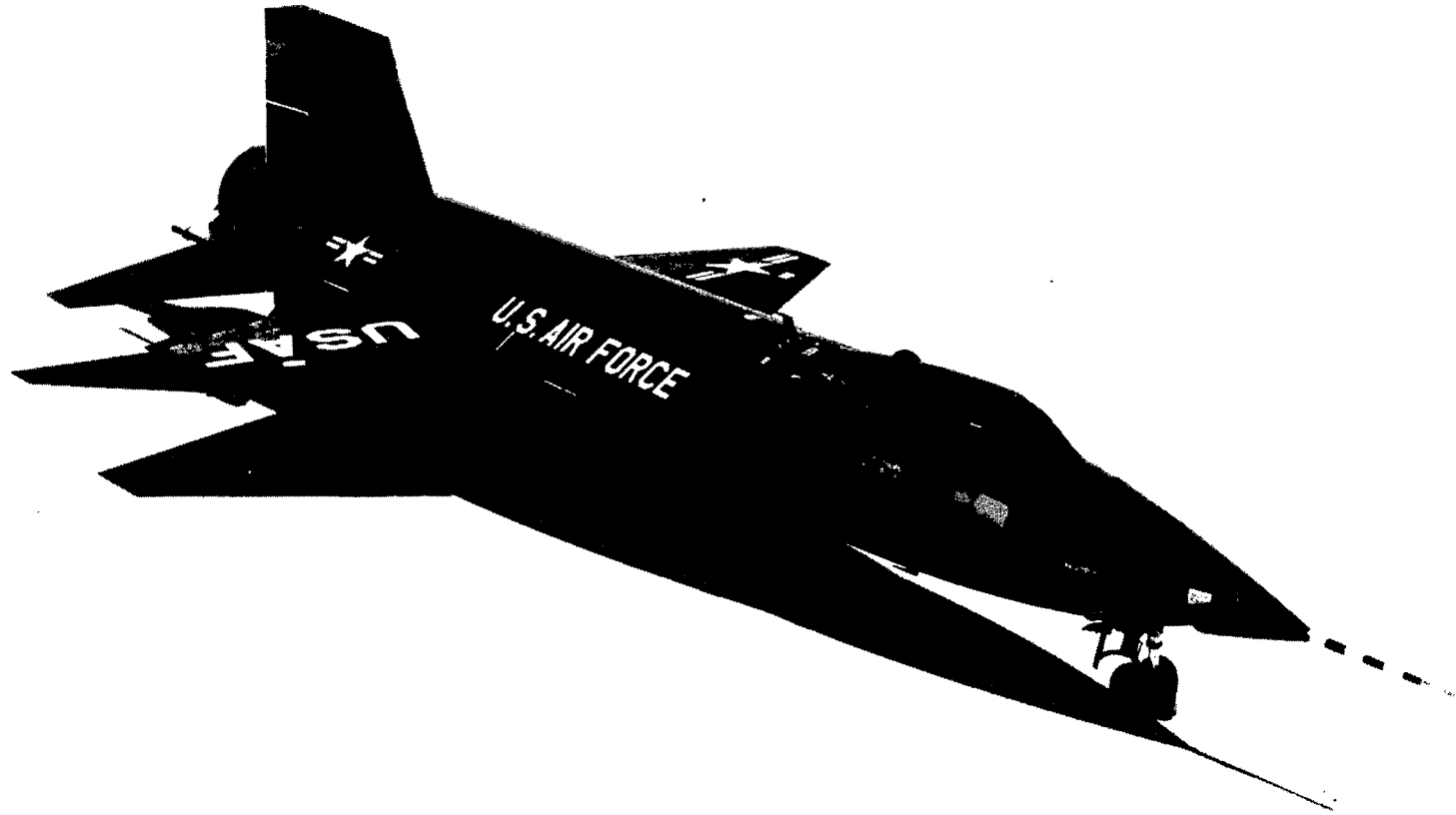
Figure 8.— X-15 airplane with nose boom.
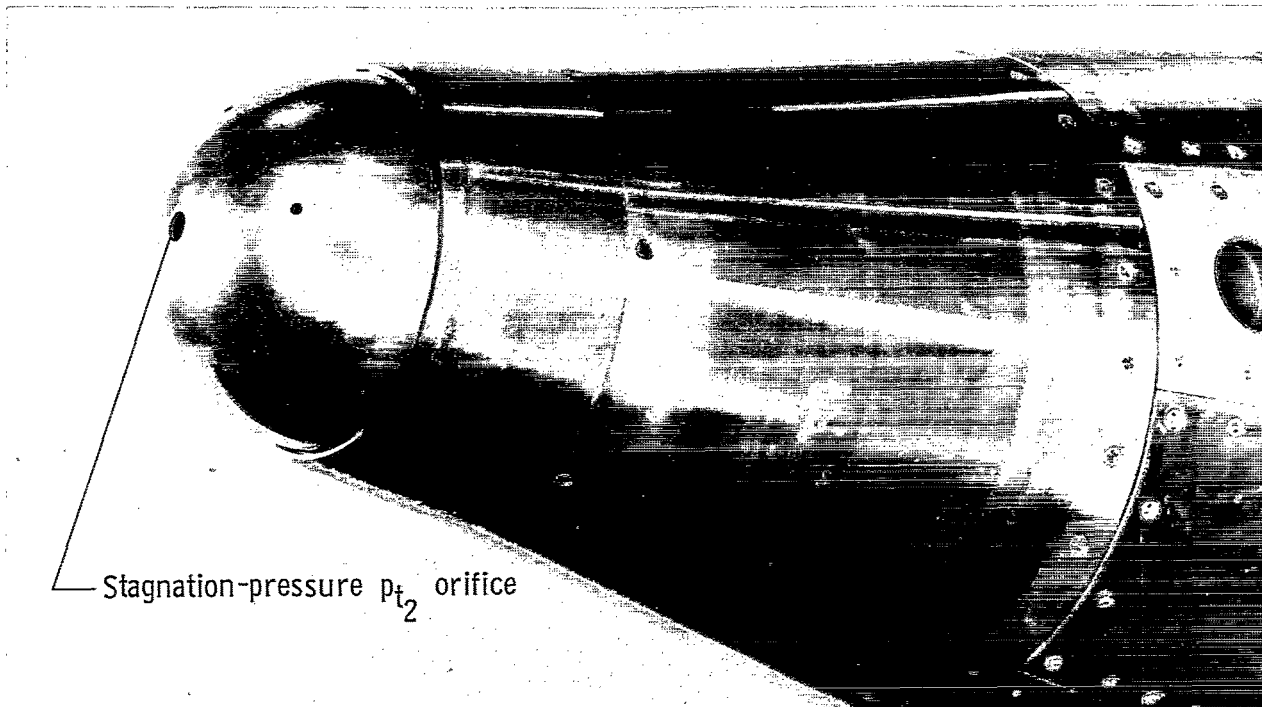
(a) Hypersonic flow-direction sensor mounted on the ogive nose of the X-15.
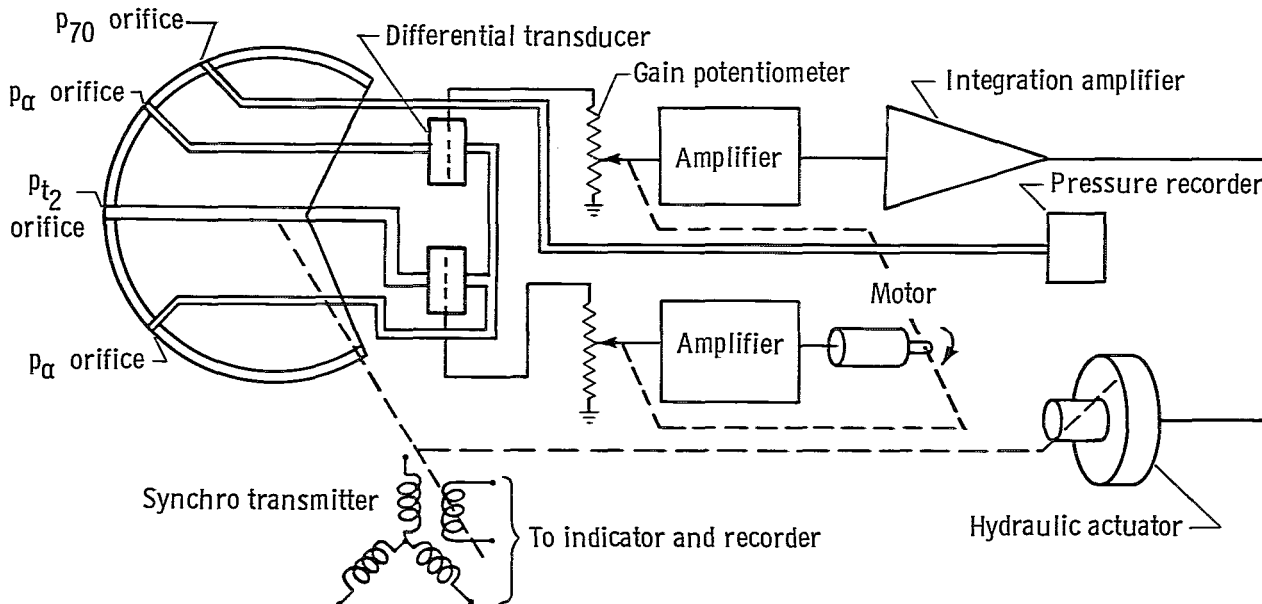
(b) Schematic of pitch plane of sensor showing basic electrical and mechanical components.

Figure 9. — X-15 hypersonic flow-direction sensor (ball nose).

Pressure instruments

Inertial instruments

Dynamic pressure (q-meter)

Three-axis ball

Velocity

Airspeed

Altitude

Altitude

Rate of climb
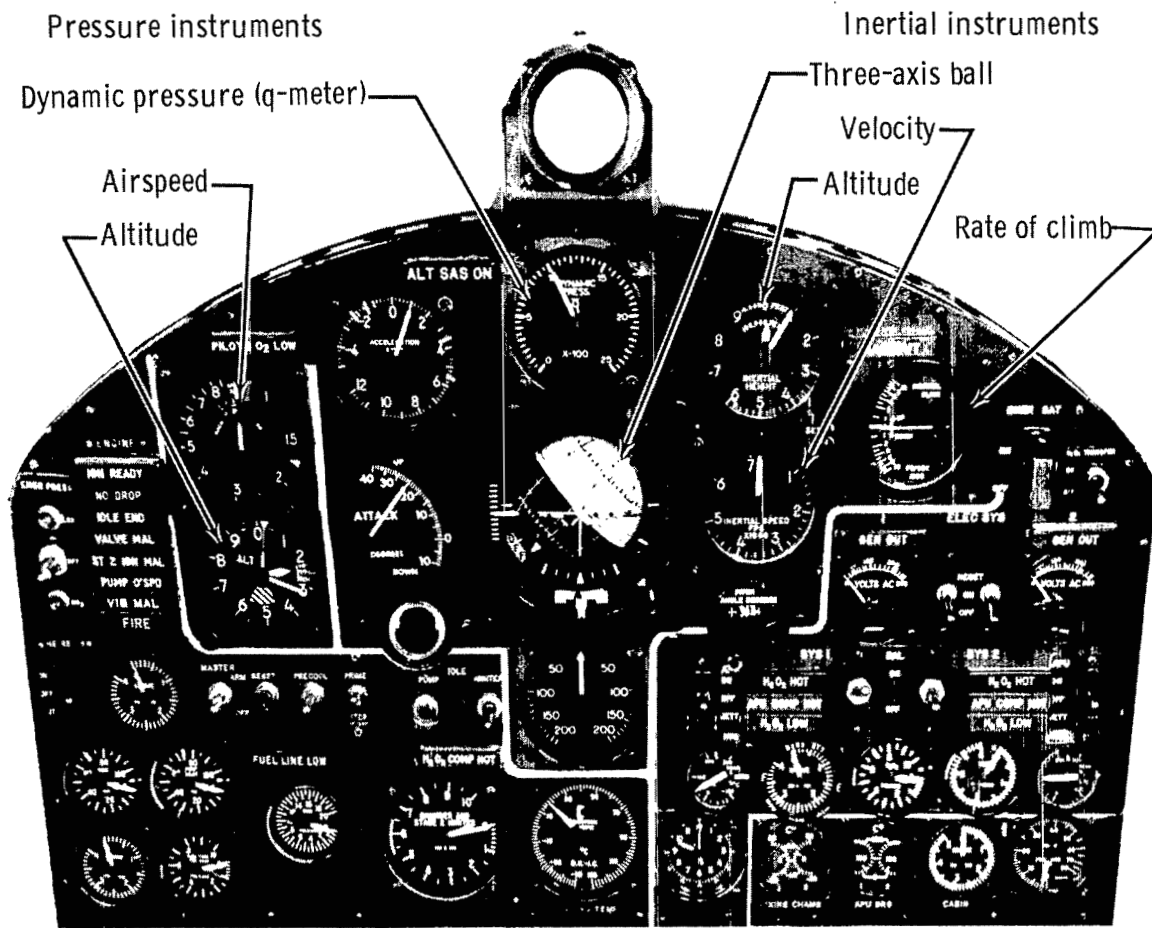
Figure 10.— X-15 cockpit panel.
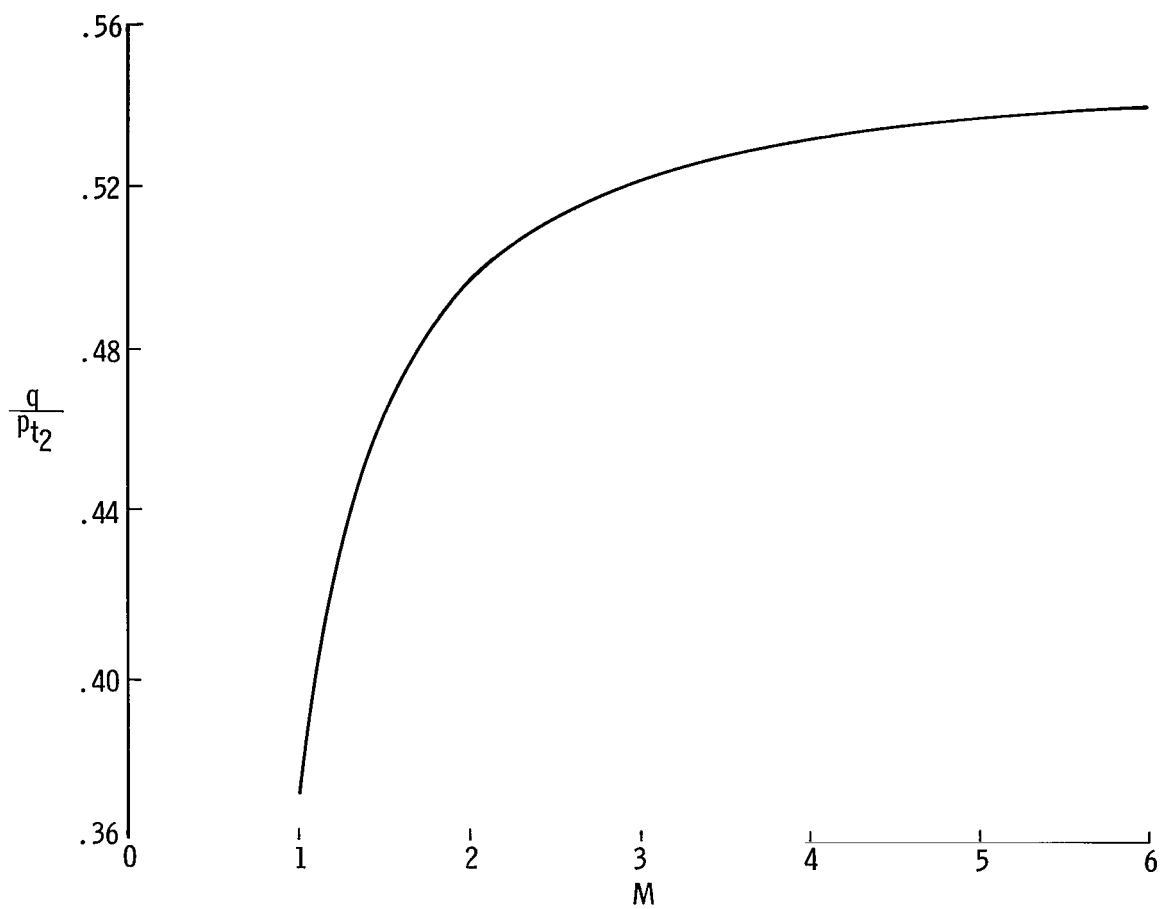
Figure 11.— The variation of $\dfrac{q}{p_{t_2}}$ with Mach number. $\gamma = 1.4$.
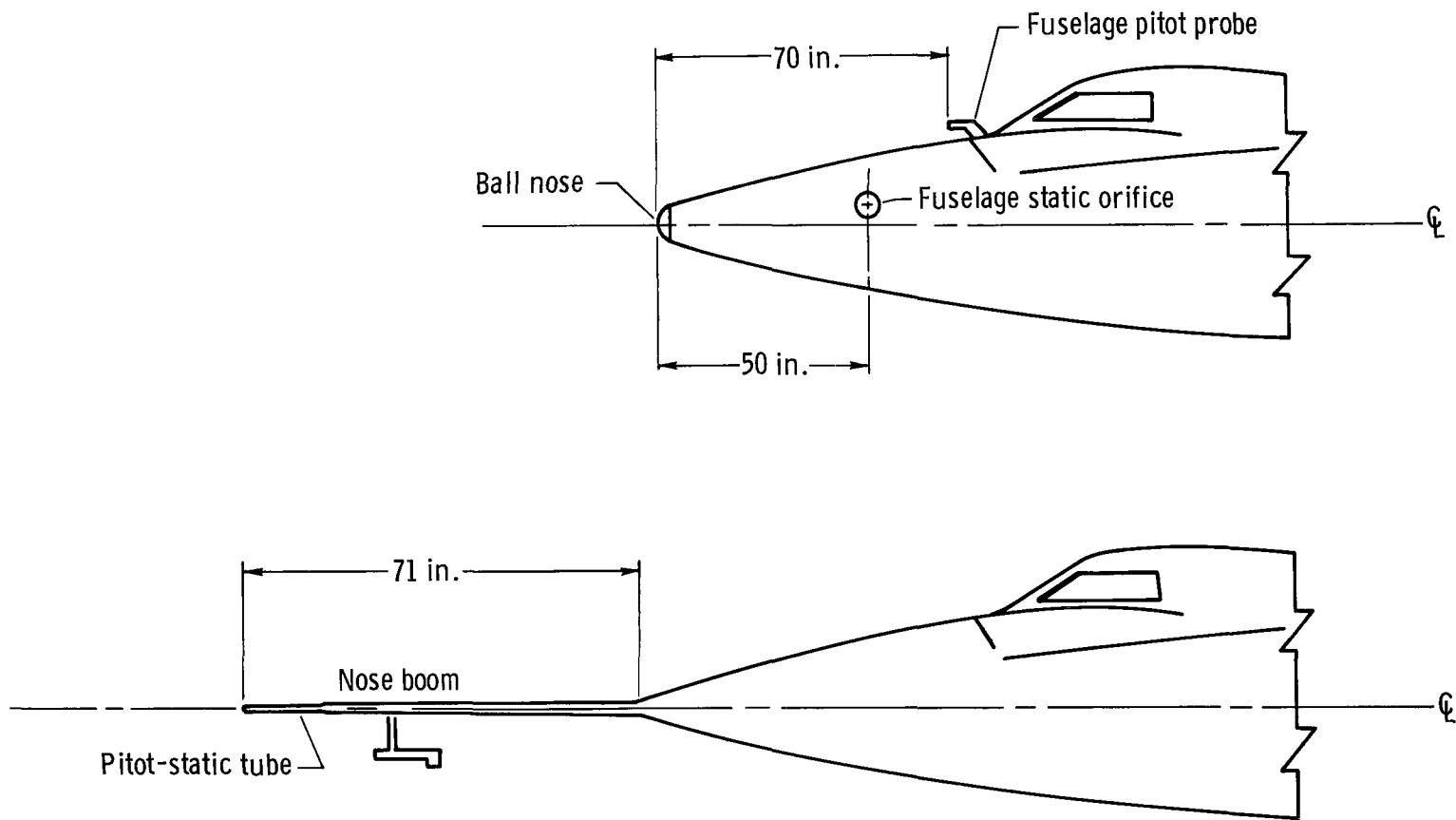
Figure 12. – Primary X-15 air-data installations.

Opening diameter   1/2 in.

2 3/4 in.
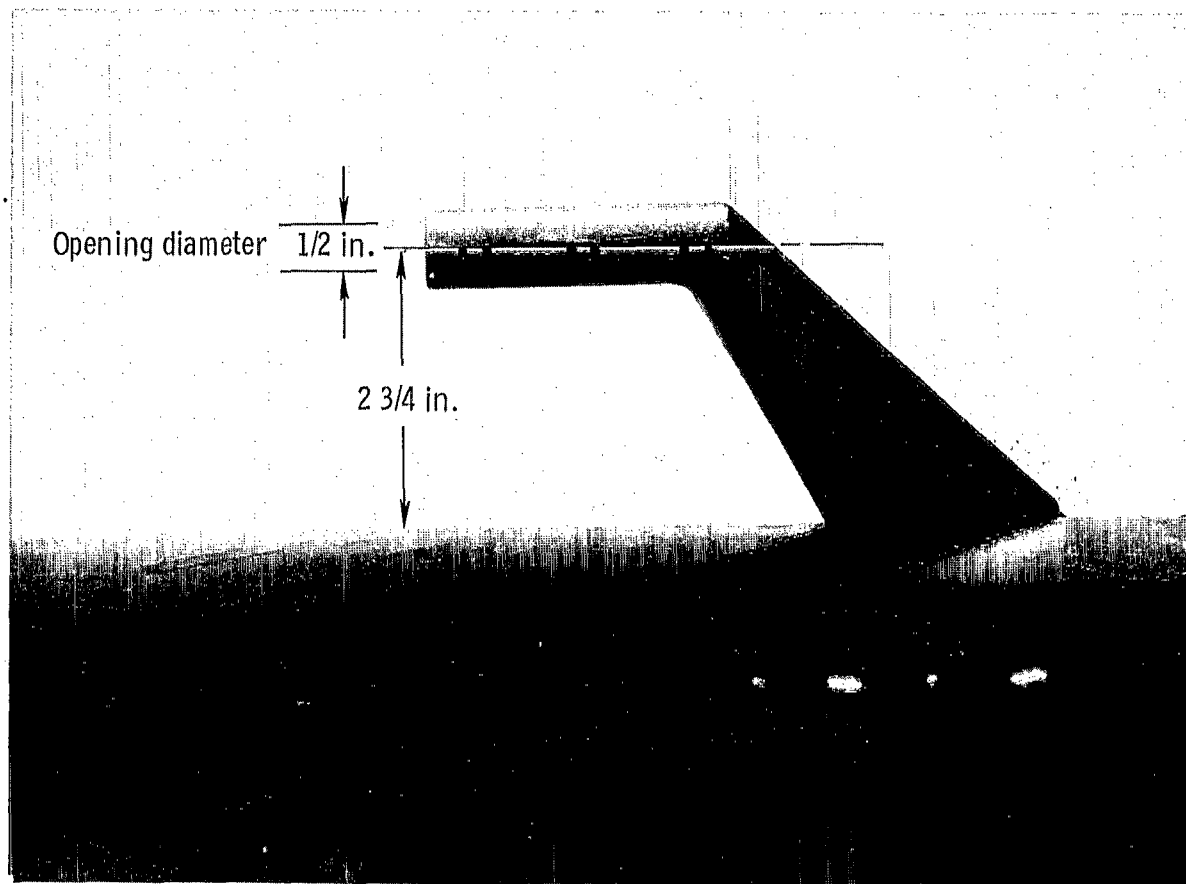
Figure 13.— Fuselage pitot probe.   (All dimensions in inches.)
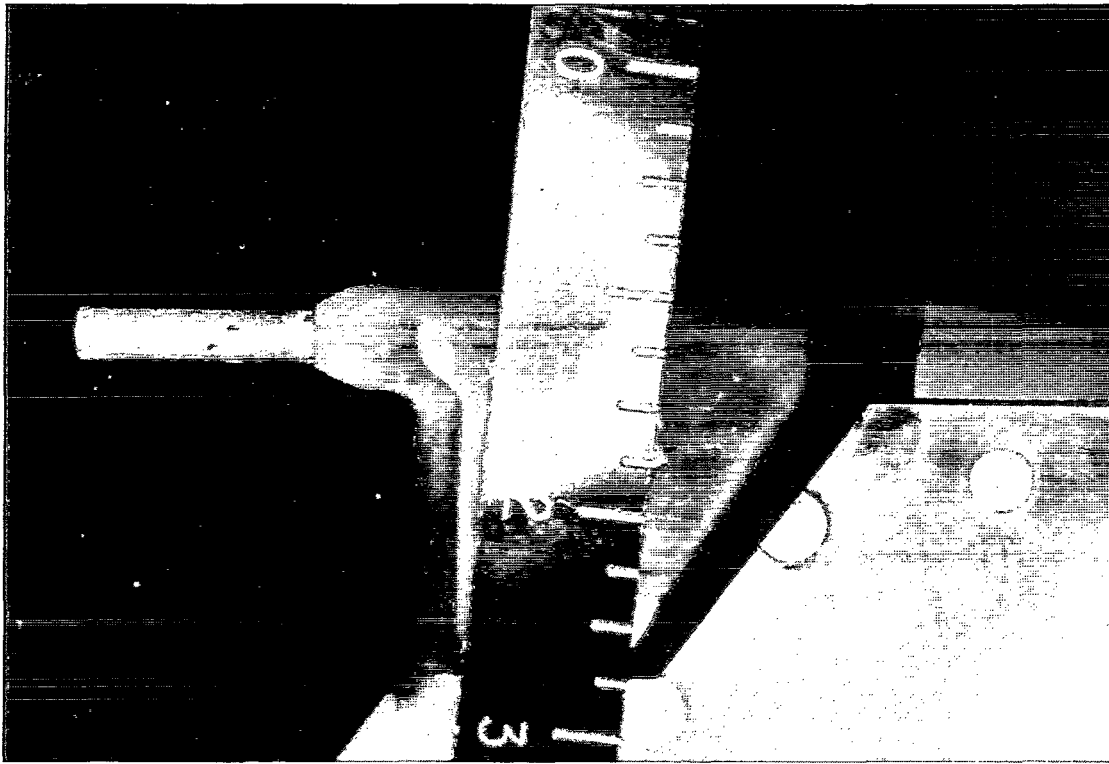
(a) Mounted on leading edge of wing tip.   Scale in inches.
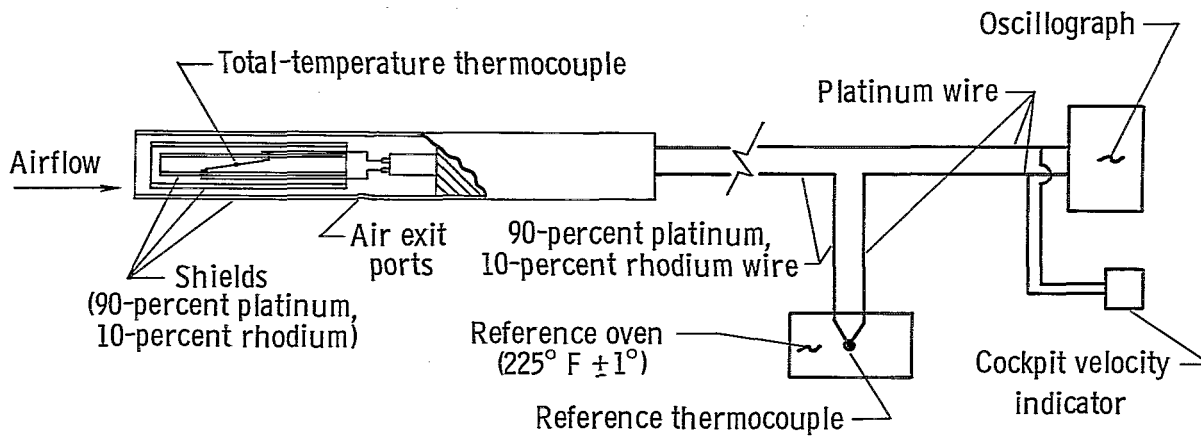
(b) Cutaway drawing and wiring schematic.

Figure 14.— Stagnation–temperature probe.
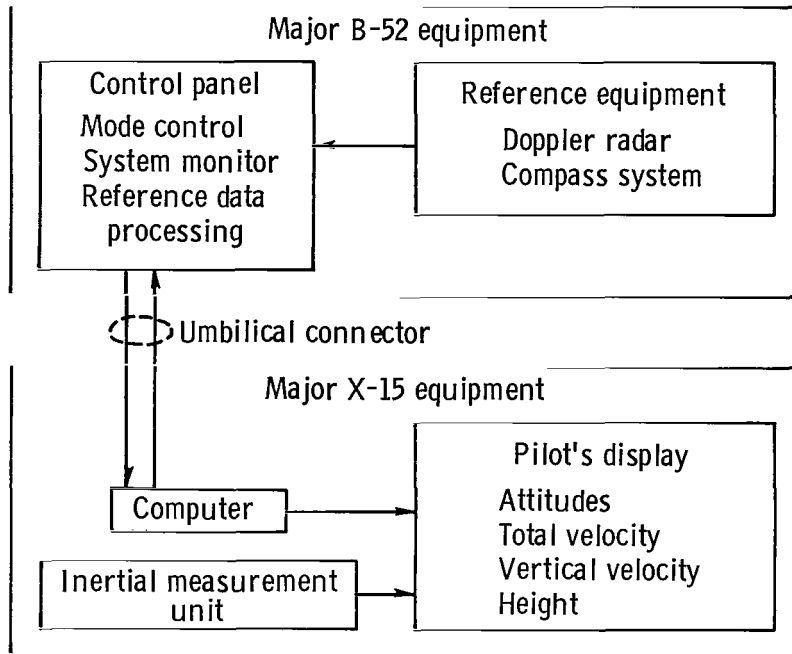
(a) Block diagram of integrated system.
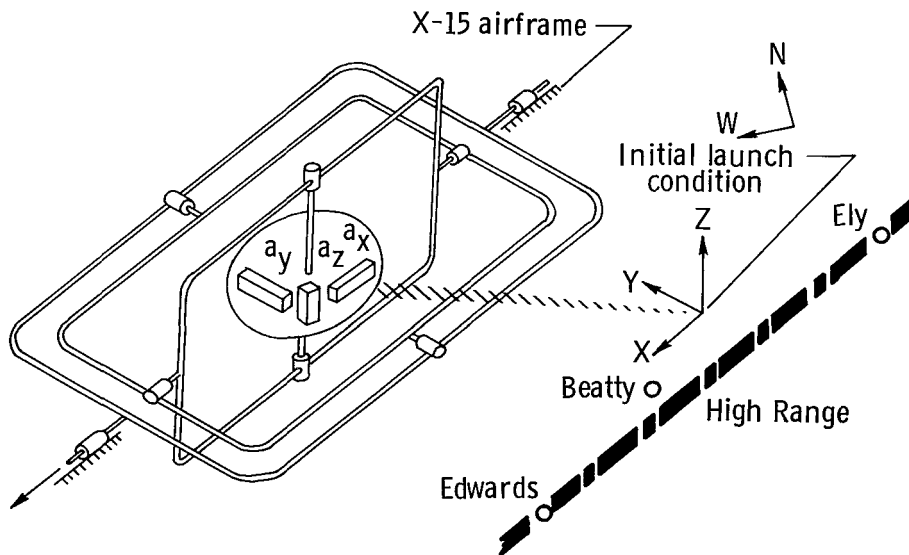
(b) Simplified sketch of inertial measurement unit and the relationship
(in azimuth) at launch to High Range.

Figure 15. — X-15 inertial flight data system.

(a) Mean January and July zonal winds for 30° N.

(b) Range of systematic variability of temperature.

(c) Departure from standard density.
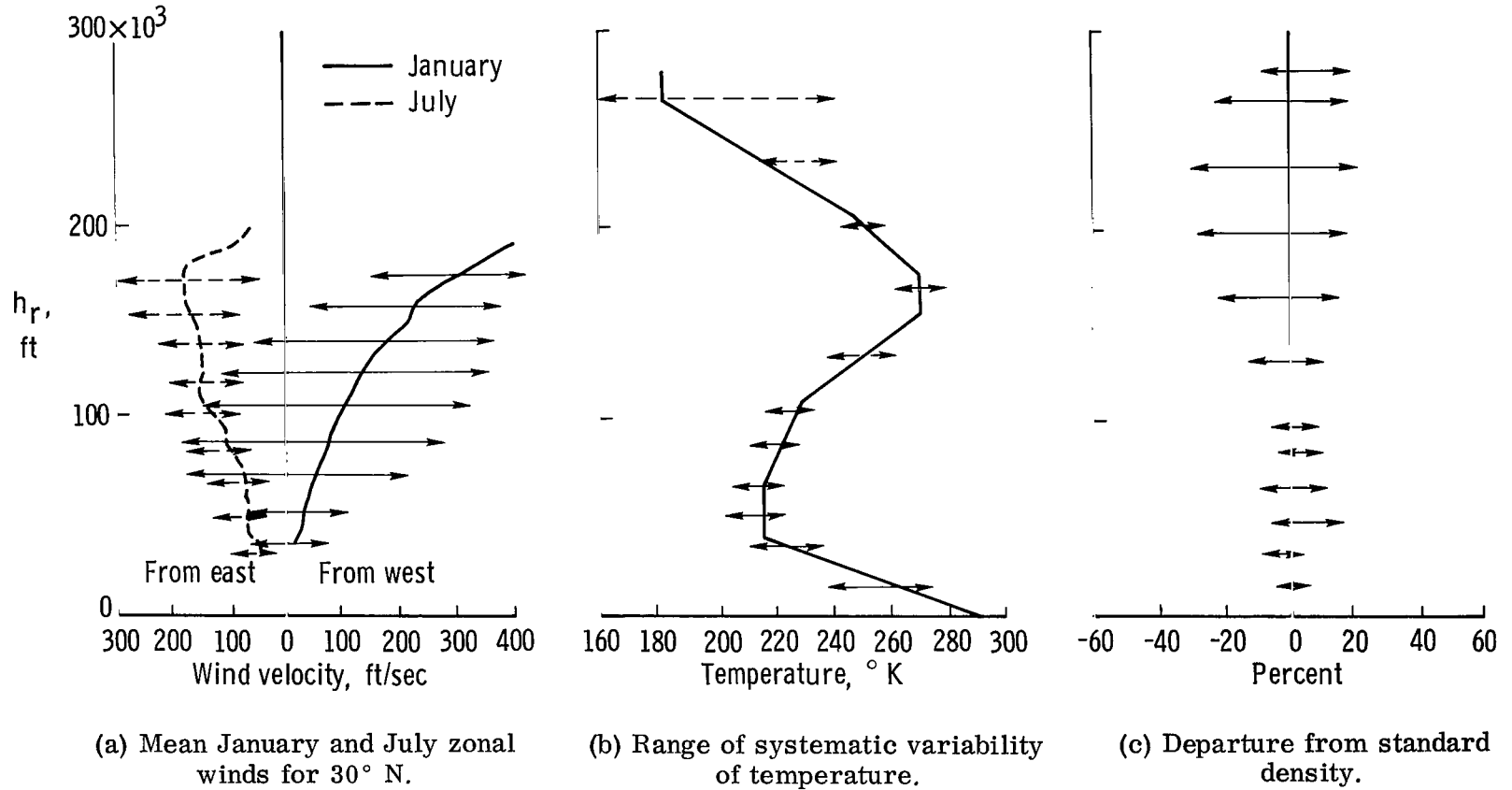
Figure 16. — Departure of winds, temperatures, and density from the U. S. Standard Atmosphere, 1962.
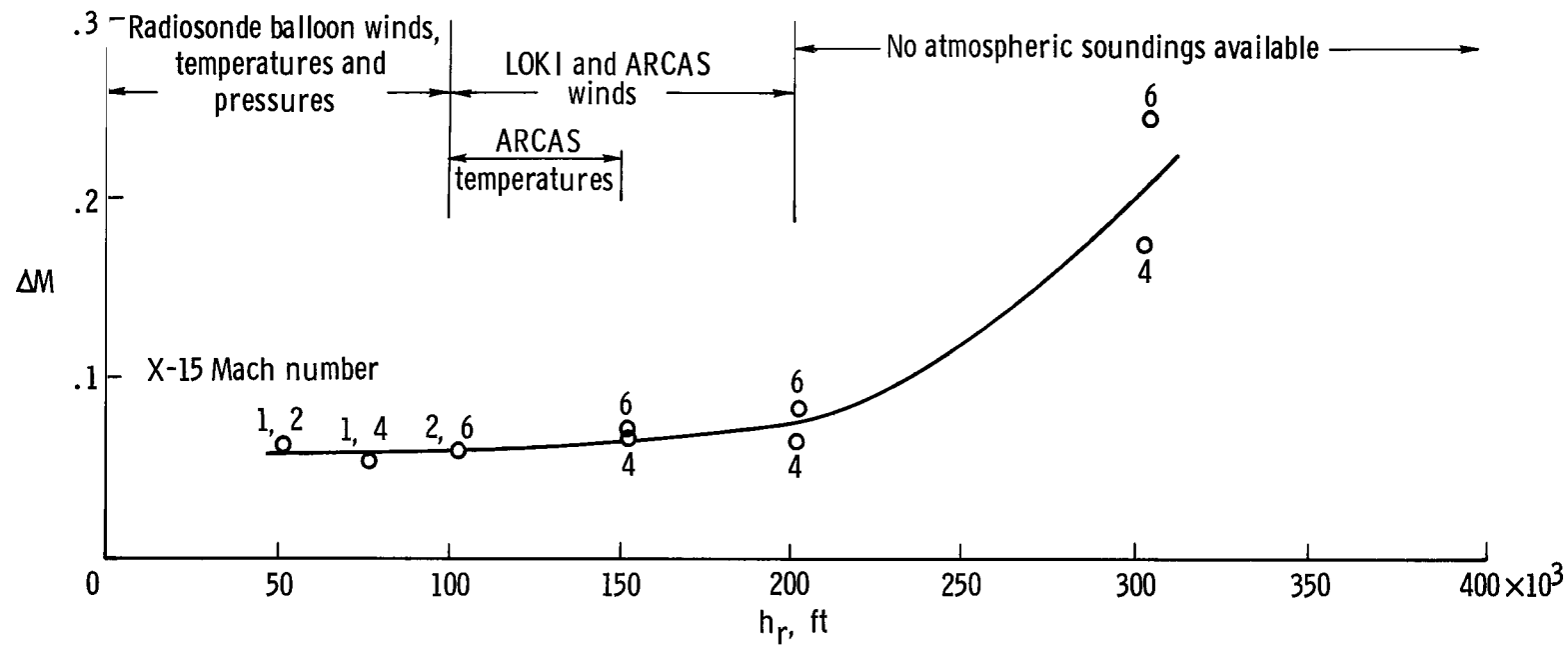
Figure 17.— X-15 Mach number error due to combined 1σ errors in meteorological parameters.
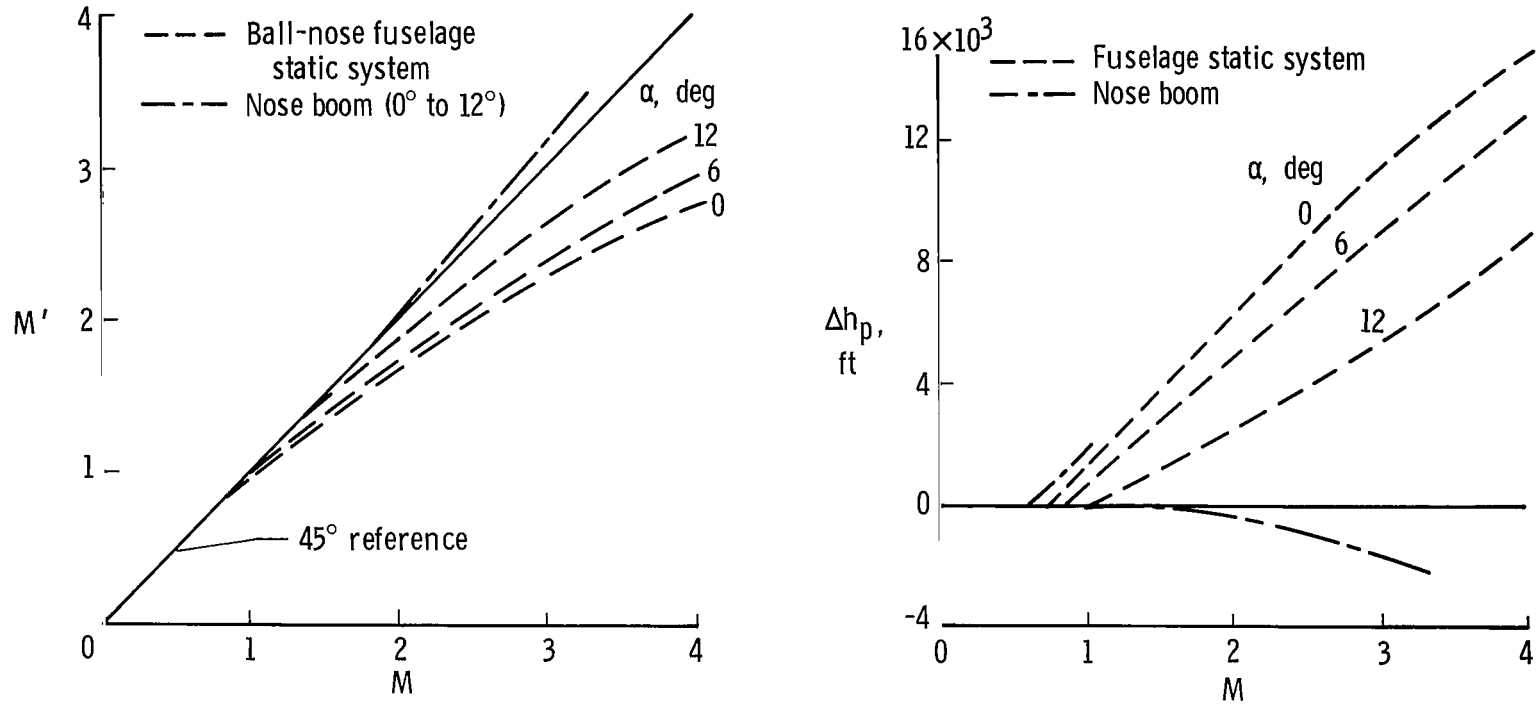
Figure 18.— Comparison of Mach number and altitude errors for two X-15 airspeed and altitude systems.
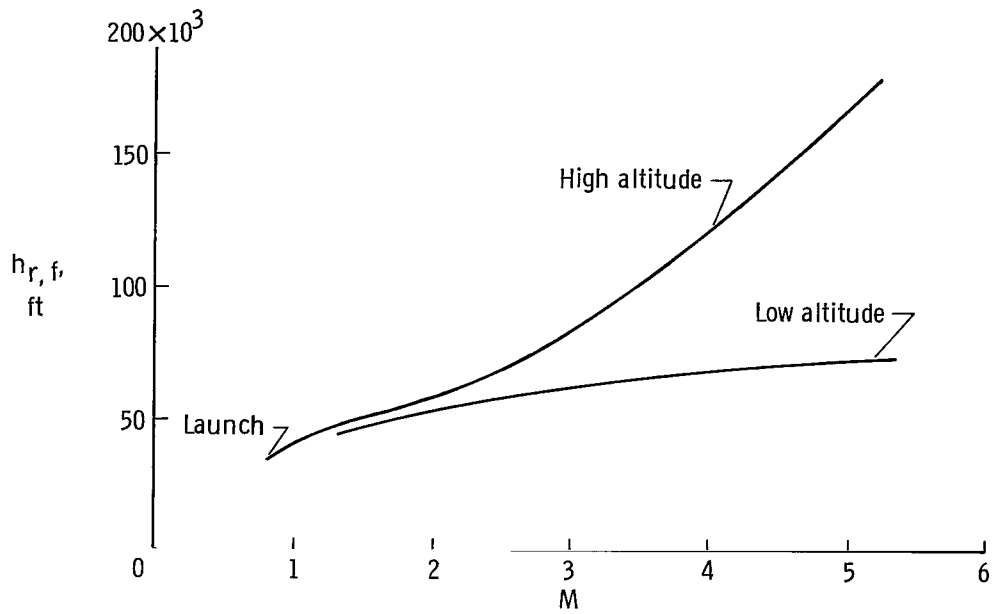
(a) Flight profile to burnout point.
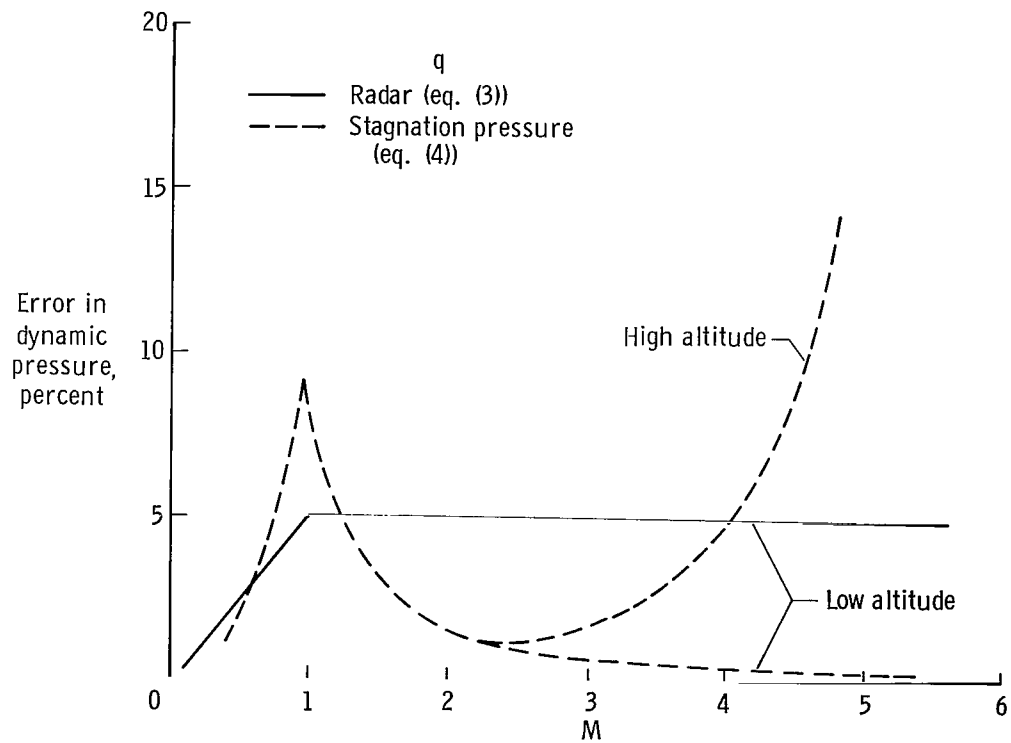
(b) Dynamic-pressure error.

Figure 19. — Dynamic-pressure errors for a high-altitude
and a low-altitude flight.
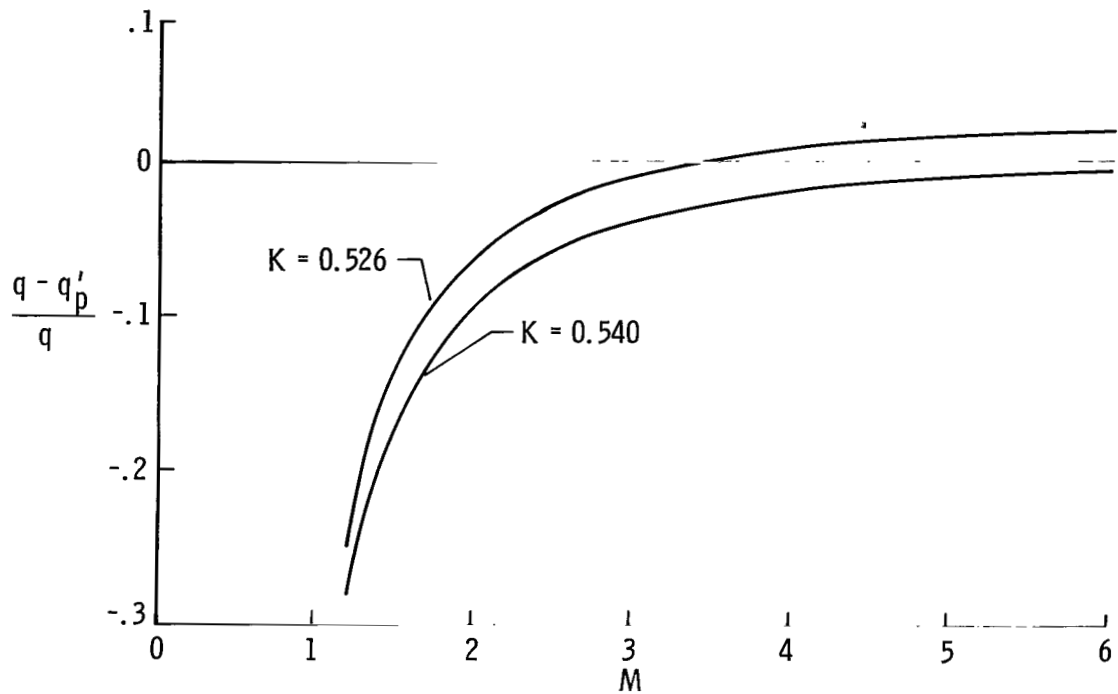
(a) Error in indicated dynamic pressure due to choice of q-meter constant.
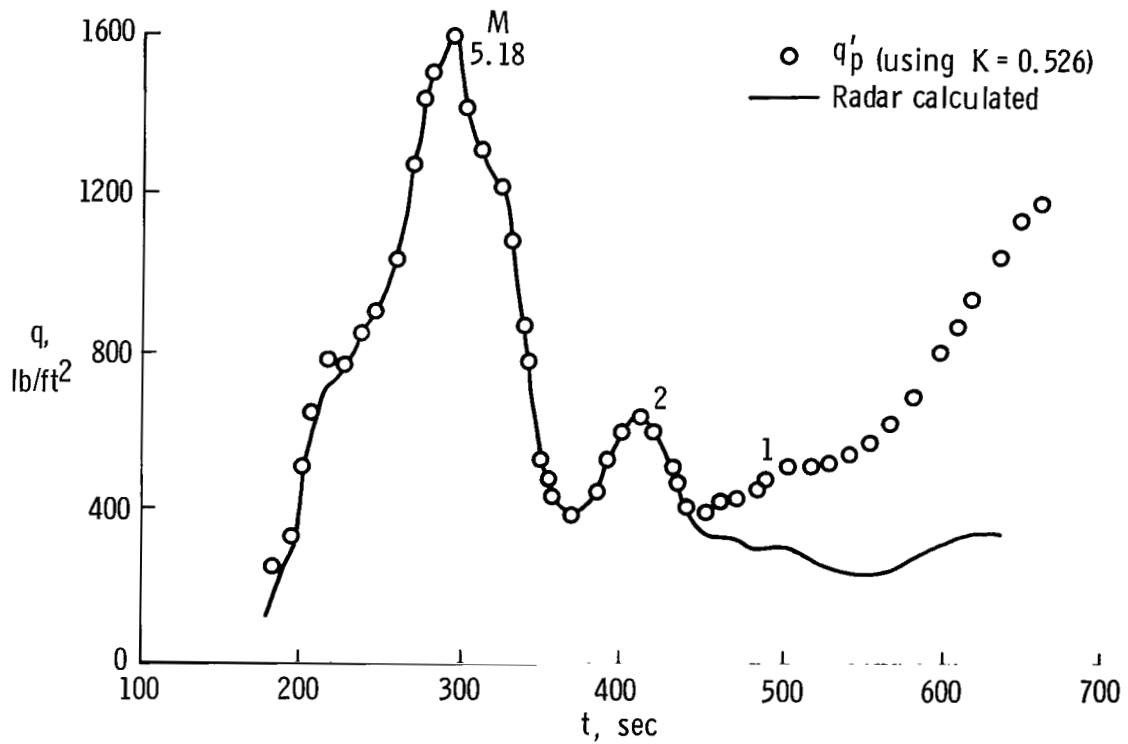
(b) Q-meter compared to radar-determined dynamic pressure.

Figure 20.— Performance of pilot's q-meter in determining
flight dynamic pressure.
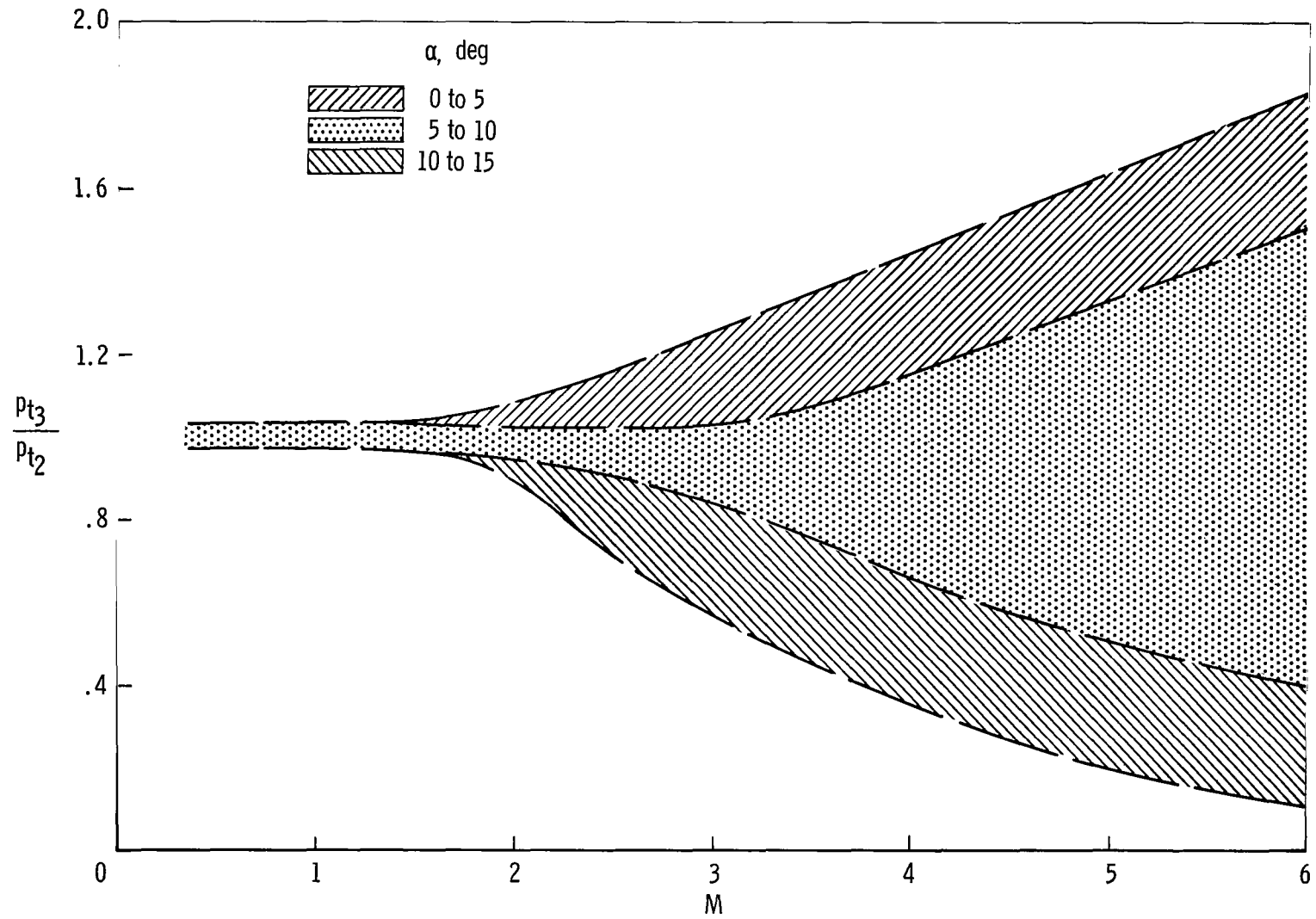
Figure 21.— Stagnation-pressure ratio of fuselage pitot probe to ball nose for differing angles of attack.
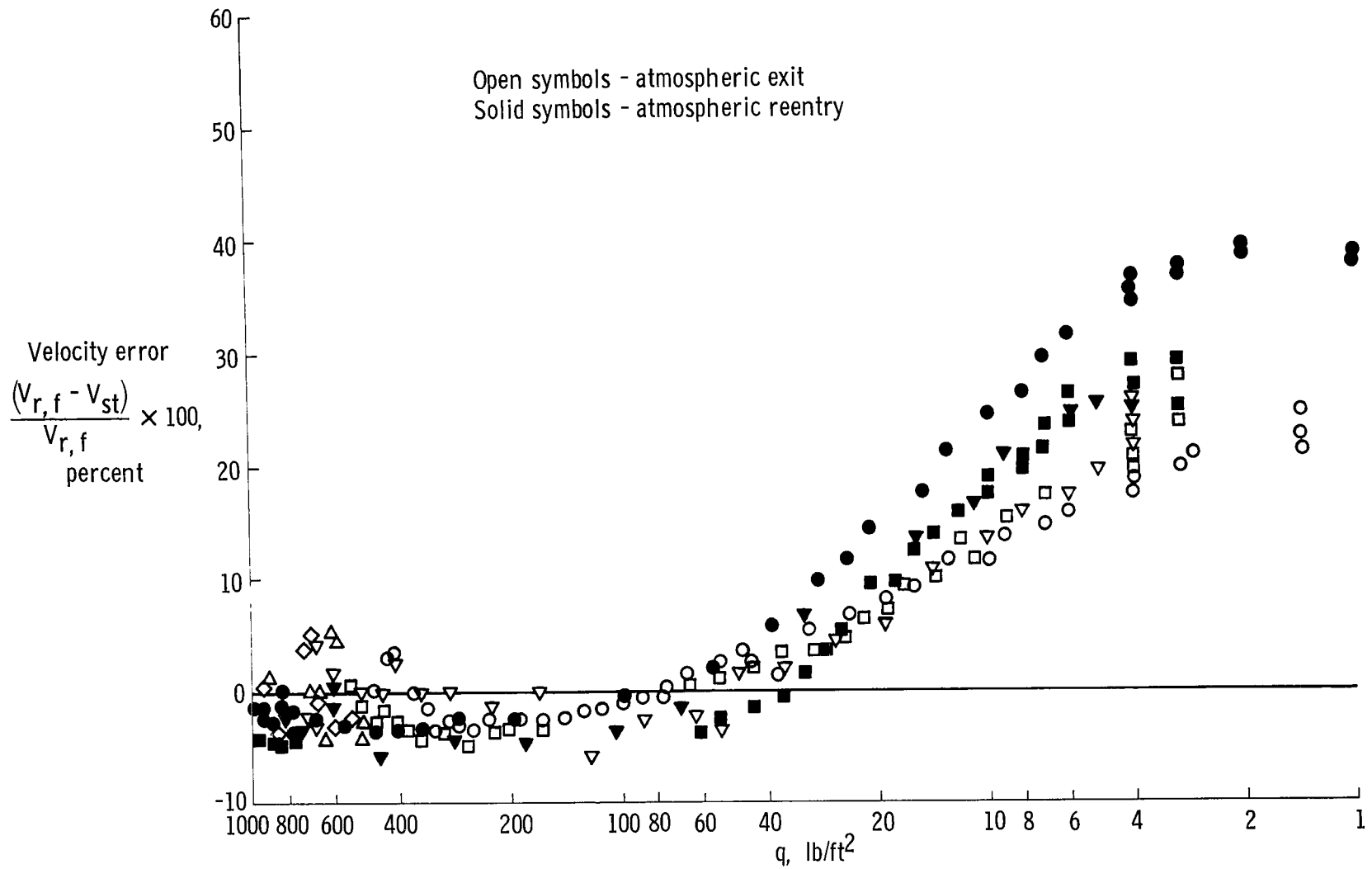
Figure 22.— Velocity errors derived from errors in stagnation-temperature measurements. Different symbols denote different flights.
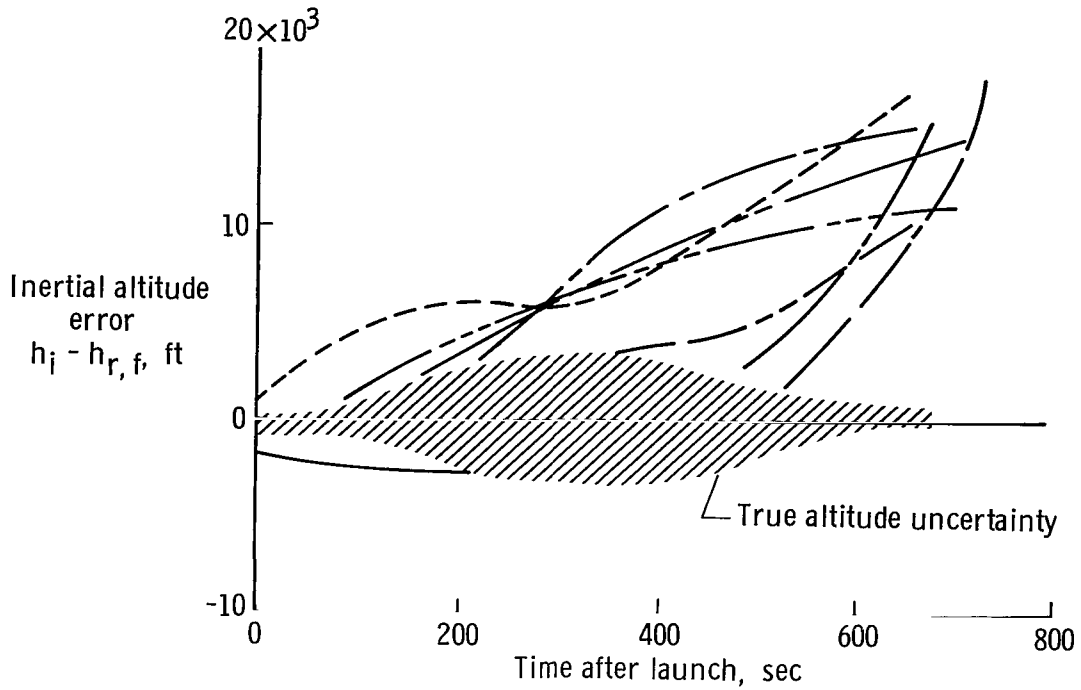
(a) Time histories of inertial-altitude errors for several high-altitude flights.
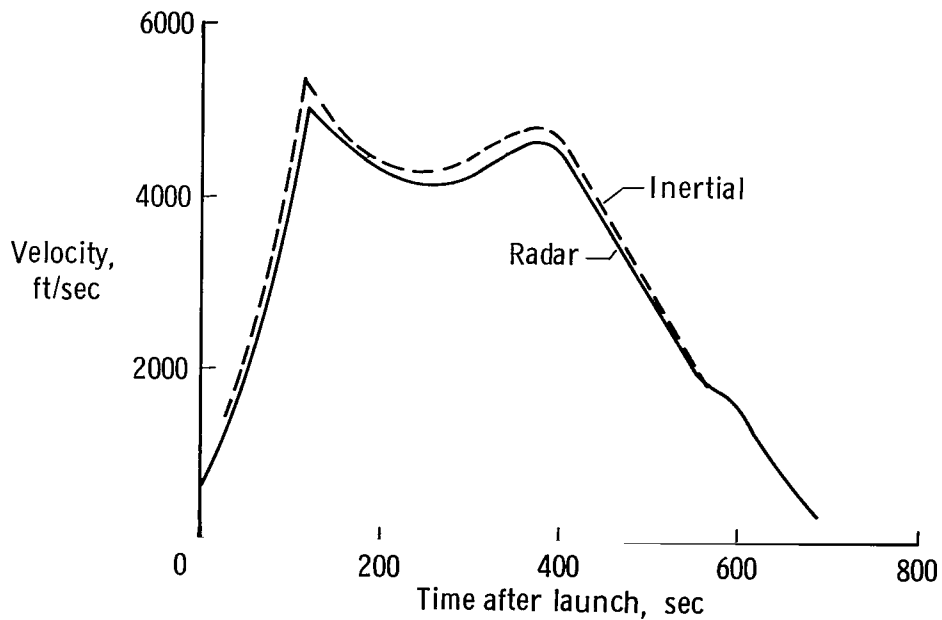
(b) Comparison of inertial and radar velocity.

Figure 23.— Inertial-platform performance during several X-15 flights.
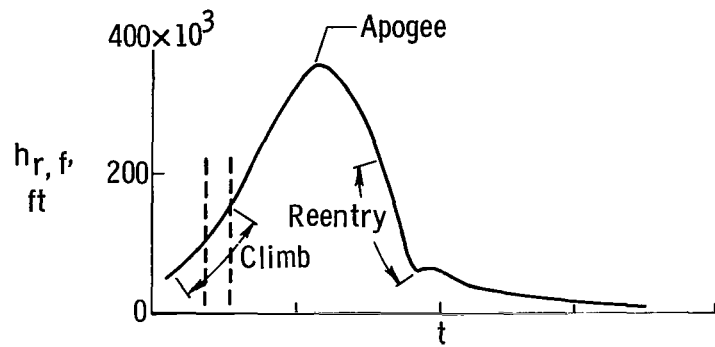
(a) High-altitude profile (ballistic trajectory).
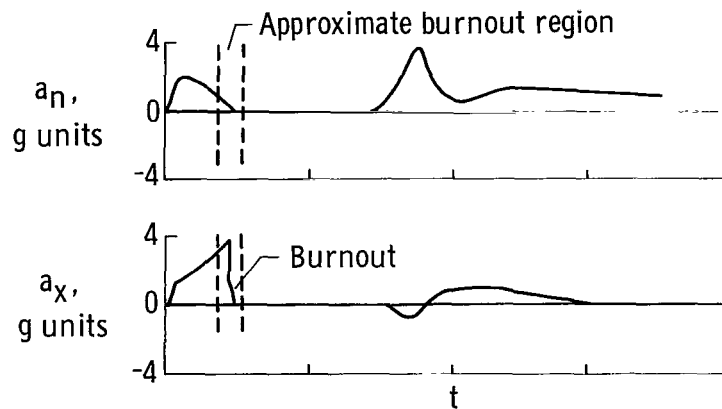
(b) Normal and longitudinal accelerations.
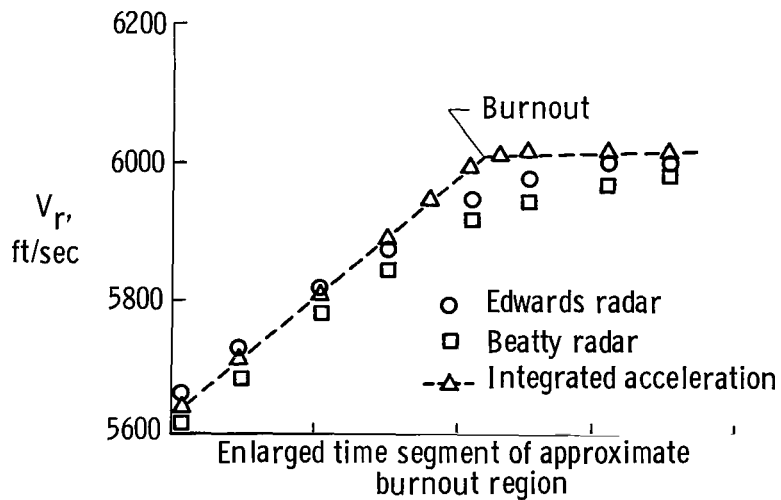
(c) Radar velocity and integrated longitudinal acceleration.

Figure 24.— Technique for determining X-15 peak velocity.
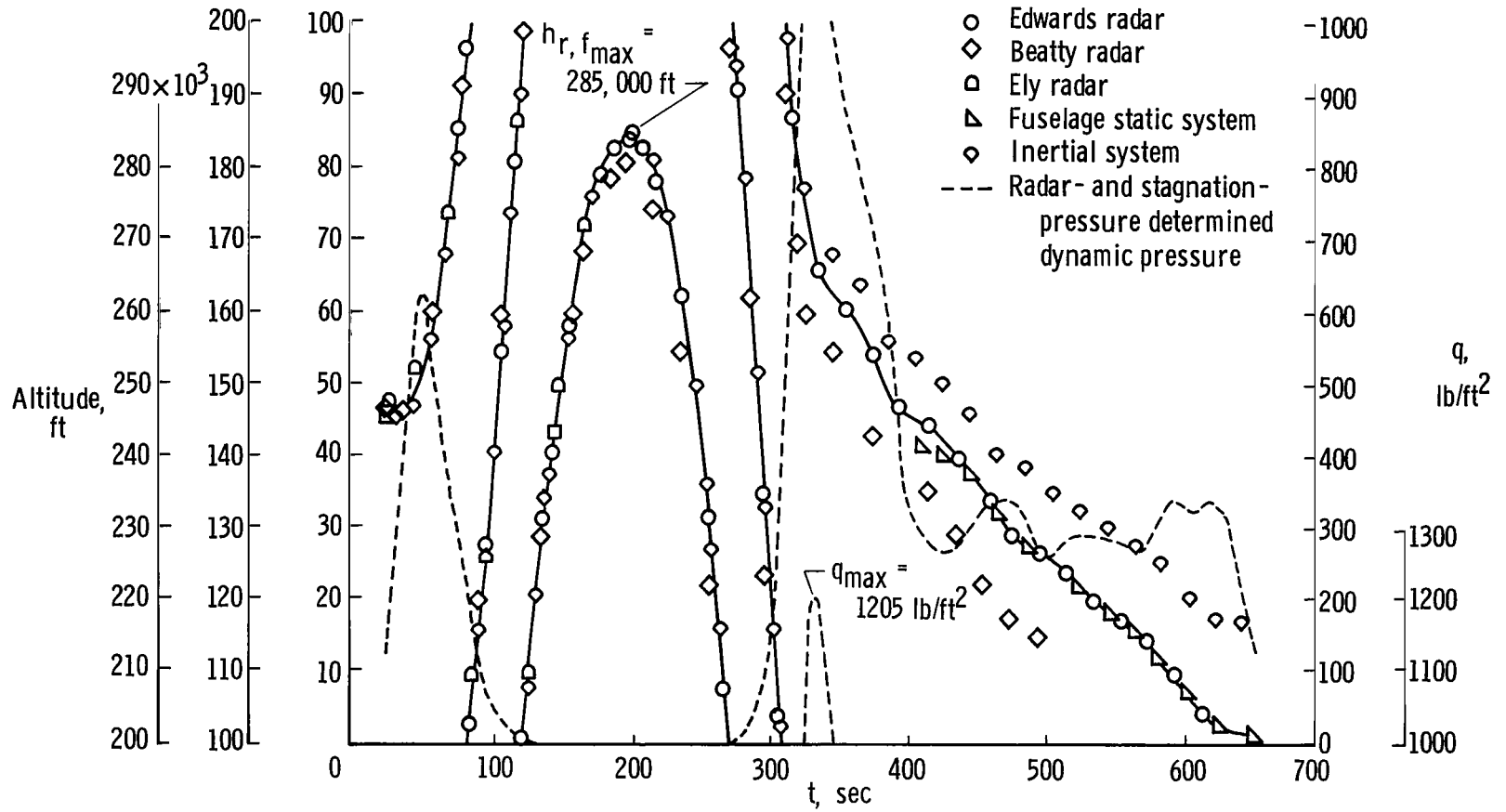
Figure 25.— Faired X-15 altitude and dynamic pressure obtained from several sources.
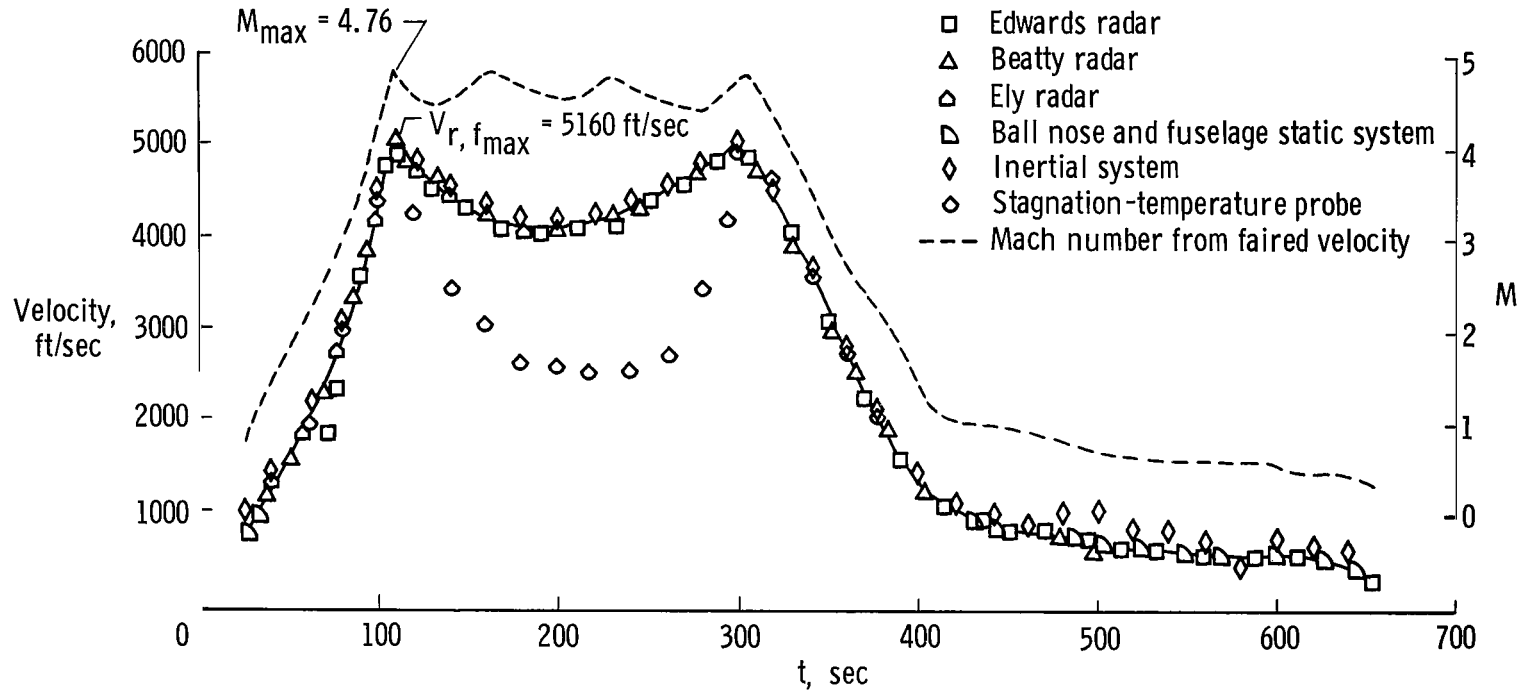
Figure 26.— Velocity data obtained from six sources, faired velocity, and calculated Mach number.
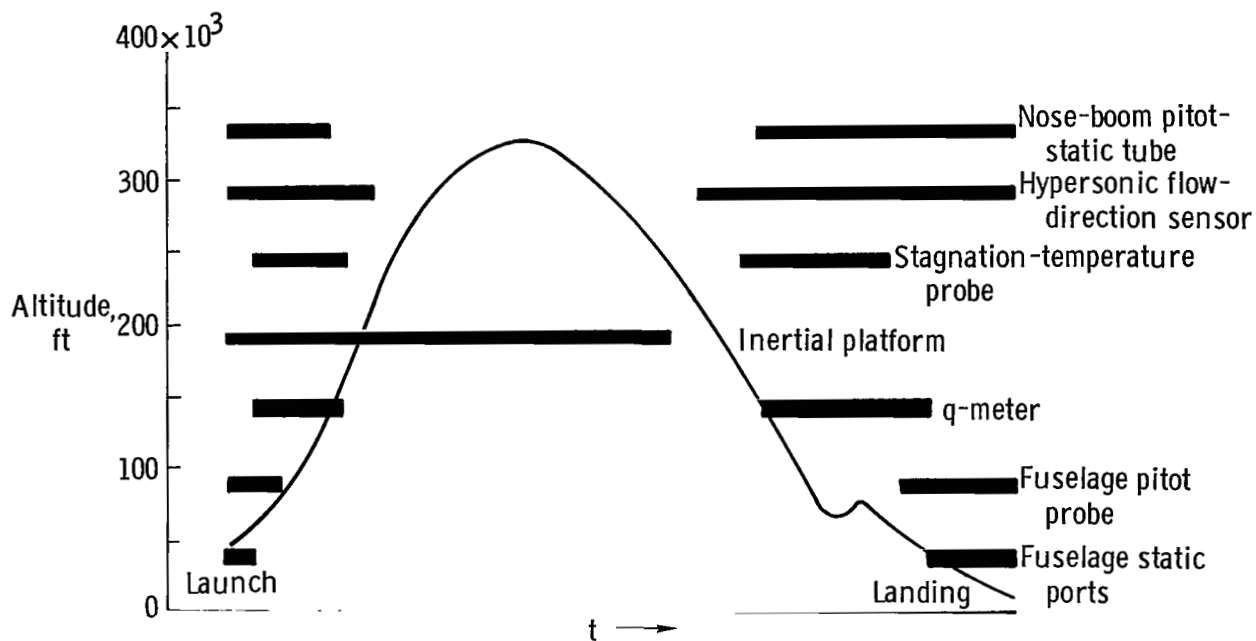
(a) X-15 high-altitude flight profile.
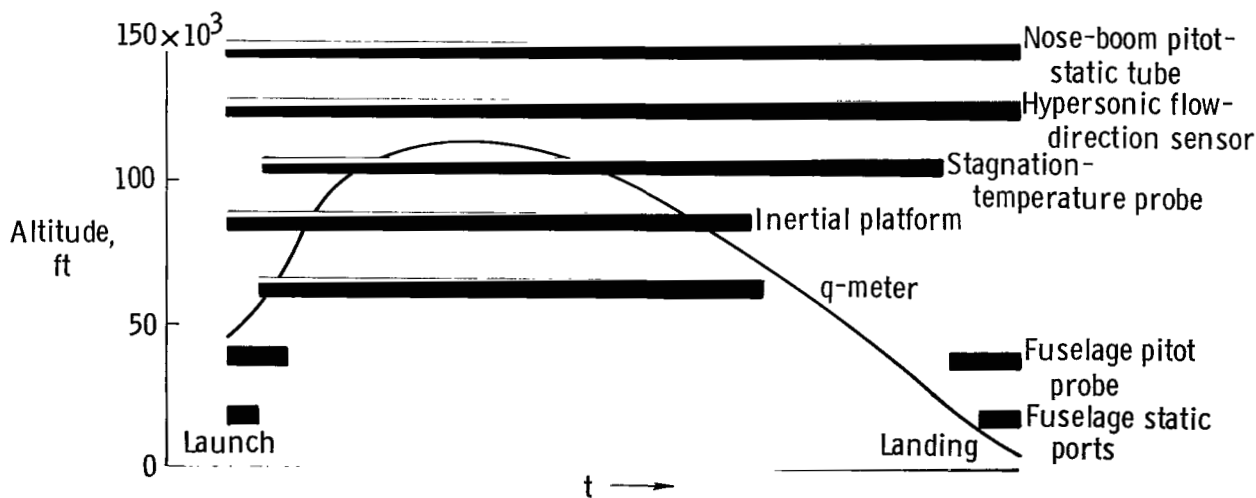
(b) X-15 low-altitude flight profile.

Figure 27. — Regions for most advantageous use of X-15 flight-
guidance sensors.

POSTMASTER: If Undeliverable (Section 158 Postal Manual) Do Not Return

"The aeronautical and space activities of the United States shall be conducted so as to contribute . . . to the expansion of human knowledge of phenomena in the atmosphere and space. The Administration shall provide for the widest practicable and appropriate dissemination of information concerning its activities and the results thereof."

— NATIONAL AERONAUTICS AND SPACE ACT OF 1958

NASA SCIENTIFIC AND TECHNICAL PUBLICATIONS

TECHNICAL REPORTS: Scientific and technical information considered important, complete, and a lasting contribution to existing knowledge.

TECHNICAL NOTES: Information less broad in scope but nevertheless of importance as a contribution to existing knowledge.

TECHNICAL MEMORANDUMS: Information receiving limited distribution because of preliminary data, security classification, or other reasons.

CONTRACTOR REPORTS: Scientific and technical information generated under a NASA contract or grant and considered an important contribution to existing knowledge.

TECHNICAL TRANSLATIONS: Information published in a foreign language considered to merit NASA distribution in English.

SPECIAL PUBLICATIONS: Information derived from or of value to NASA activities. Publications include conference proceedings, monographs, data compilations, handbooks, sourcebooks, and special bibliographies.

TECHNOLOGY UTILIZATION PUBLICATIONS: Information on technology used by NASA that may be of particular interest in commercial and other non-aerospace applications. Publications include Tech Briefs, Technology Utilization Reports and Notes, and Technology Surveys.

Details on the availability of these publications may be obtained from:

SCIENTIFIC AND TECHNICAL INFORMATION DIVISION

NATIONAL AERONAUTICS AND SPACE ADMINISTRATION
Washington, D.C. 20546